Physics – Uspekhi **40** (9) 899 – 924 (1997)

REVIEWS OF TOPICAL PROBLEMS PACS numbers: **61.46.+w**, **85.42.+m**

Carbon nanotubes

A V Eletskiĭ

Contents

Abstract. A review is presented of the current knowledge of carbon nanotubes — cylindrical particles made of one or several concentric graphite layers. Nanotube fabrication techniques are considered and possible nanotube structures analyzed. Data on their electrical and magnetic properties are presented. The relation between nanotube electrical properties and structure (in particular, chirality) is emphasized. Potential applications in nanoelectronics and other active areas of research and technology are discussed.

1. Introduction

The discovery of fullerenes in 1985 [1], the awarding of the Nobel Prize for Chemistry in 1996, as well as the development of the technology for their production in macroscopic amounts [2] have given a start to the systematic research of surface carbon structures. The principal element of such structures is the graphite layer, i.e. a surface inlaid with regular hexagons at vertices of which are situated carbon atoms. In the case of fullerenes [1 – 3] such a surface has a closed spherical or spheroidal shape. The surface structure of fullerenes contains not only regular hexagons, whose number depends on the fullerene size, but also 12 pentagons arranged in a regular manner over the surface. The variety of unusual physical and chemical properties of fullerenes as well as promising prospects for their possible applications are attracting the steadily growing interest among researchers from different fields of science and production engineering.

Besides spheroidal structures graphite layers can also form lengthy structures such as the hollow cylinder [4]. These structures referred to as nanotubes are also distinguished by a wide diversity of physical and chemical properties and receive widespread attention from researchers and technologists. In this article methods of generation, the structures, and main physical and chemical properties of carbon nanotubes are reviewed. Possible mechanisms for nanotube formation are analyzed. The problems related to the practical application of this new material are considered as well.

The story of carbon nanotube discovery is closely connected with that of the disclosure and detailed investigation of fullerenes. The latter was made possible as a result of the development of the technology for producing fullerenes in macroscopic quantities by W Kraetschmer, D Huffman et al. [2]. This technology is based on the thermal deposition of graphite in an electrical arc with graphite electrodes in the helium atmosphere. As a result of graphite deposition a soot is formed, which covers the walls of a gas discharge chamber and contains up to 20% fullerenes, mainly C_{60} and C_{70}. Unlike others components of soot, fullerenes dissolve in organic solvents (benzene, toluene, etc.) and can be extracted, purified and separated using liquid chromatography.

Shortly after the fullerene production technology was developed it was found [4] that as a result of the thermal sputtering of a graphite anode in an electrical arc not only molecules belonging to the fullerene family form, but also elongated structures, which represent graphite layers scrolled

A V Eletskiĭ Russian Research Centre 'Kurchatov Institute',
pl. Kurchatova 1, 123182 Moscow, Russia
Tel. (7-095) 196-72 80
E-mail: eletskii@mail.imp.kiae.ru

Received 30 June 1997
Uspekhi Fizicheskikh Nauk **167** (9) 945 – 972 (1997)
Submitted in English by the author; edited by A Radzig

into a single-layer or multilayer tube. These structures, called 'nanotubes', can reach tens of microns in length, which is several orders of magnitude in excess of their diameter usually ranging from one to several nanometers. Unlike fullerenes, which are deposited together with soot on a gas discharge chamber wall, nanotubes are found predominantly on the cathode surface facing the interelectrode gap. As is evident from electron microscope observations, the majority of nanotubes consist of a number of scrolled graphite layers, which are either one inside another or wrapped around a common axis. The spacing between layers is usually 0.34 nm, which is the interlayer spacing in crystalline graphite. Nanotubes usually end with a hemispherical cap, which also includes regular pentagons in its structure with the hexagons and looks like a half of a fullerene molecule. It is of interest to note that the possibility of the existence of carbon nanotubes was predicted for the first time by authors of the theoretical work [5], where among other things their possible electronic properties were also calculated. It is significant that in the work cited special attention is given to the possible metallic conductivity of nanotubes and the absence of any forbidden band. However the publication of this work was initially rejected, and it was accepted for publication only after publishing the experimental work [4], where nanotubes were firstly produced and observed.

In the initial experiments the content of nanotubes in a deposit covering the cathode surface did not exceed several percent. However, further modification of the technology resulted in a rise of the nanotube yield up to tens of percent [6, 7]. The vast majority of nanotubes observed in the first experiments made multilayer structures which differed in the number of layers, the shape of the ending cap and some other characteristics. This peculiarity hindered the detailed study of nanotube properties, because these properties relate to a specific sample rather than to bulk nanotube material.

A difference in the chemical activity of a cylindrical wall of nanotube and its spherical cap permitted the development of methods to control the nanotube parameters using the partial oxidation of a nanotube [8, 9]. These methods offer a possibility to produce nanotubes with open ends as well as single-layer nanotubes. The latter initiated the development of the study of nanotubes with given characteristics. Further development of the technology for the production of nanotubes with specified parameters is based on the use of catalysts [10], which are usually the transition group metals. This approach has permitted the production of samples containing mainly single-layer nanotubes and finally resulted in the creation of material consisting predominantly of single-layer nanotubes of the same radius [11]. It should be noted that along with a graphite-electrode electrical arc, the electrolytic method is used quite effectively for the nanotube production in macroscopic quantities [12 – 14].

Carbon nanotubes combine both molecular and solid state properties and can be considered as an intermediate state of substance. This peculiarity attracts a steadily rising interest from researchers addressing the basic features of behaviour of such an exotic object in various conditions. Those features of considerable scientific interest can be used as a basis for effective practical applications of nanotubes in wide fields of science and technology.

Already the first carbon-nanotube experiments revealed their unusual properties which appear to be atypical for nanosize objects. Thus, open nanotubes show capillarity effects [15] and can take in molten metals and other liquids. This property of nanotubes has offered the prospect of creating conductive threads of nanometer diameter, to form the basis for new electronic devices of nanometer size. Recently [16] the possibility of the incorporation of superconducting material (TaC) inside the nanotube was shown. As indicated by the experimental data, this incorporated material does not lose its superconducting properties at $T < 10$ K. The variety of theoretical calculations [17 – 24] indicate that the electrical properties of an individual nanotube are determined to a considerable degree by its chirality, i.e. the orientation angle of a graphite plane relative to the axis of a tube. Depending on the chirality, a single-layer nanotube can be like either graphite, semimetal, which has no energy gap, or semiconductor, whose energy gap ranges between 0.01 and 0.7 eV. The connection of two nanotubes with different chiralities and therefore different electronic characteristics represents a p – n heterojunction several nanometers in size and could be also used as the base for a next generation electronic device [25, 26]. As follows from direct measurements [27 – 29], nanotubes have quite a high emission capability: the room temperature field-emission electron current density reaches about 0.1 A cm^{-2} at an applied voltage near 500 V. This offers one more interesting possibility for the practical use of nanotubes in electronics.

The quite high mechanical strength of carbon nanotubes in combination with their conductivity provides a possibility for their application as the probe in a scanning microscope, designed to study the finest surface nonuniformities [30]. It can enhance the resolution of such devices by as much as several orders of magnitude and make them comparable with such a unique facility as the field-ion microscope. The use of nanotubes in chemical technology has notable prospects as well. One possible direction here, based on the high specific area combining with the chemical stability of carbon nanotubes, relates to the use of nanotubes as a support in heterogeneous catalysis. The results of preliminary experiments [31] show the anomalous high catalytic activity of nanotubes in the liquid phase hydrogenation of *p*-nitrotoluene and gas phase hydrogenation of CO in the presence of Ni and Pr nanoparticles, incorporated into the nanotube substance.

Thus, carbon nanotubes represent a new physical material with unique properties, which may find effective application in a variety of scientific and technological fields. This review is devoted to the detailed consideration of the indicated properties and the analysis of prospects for possible applications of carbon nanotubes. The methods of production of carbon nanotubes under various conditions are reviewed. And the most important experiments determining the main properties of carbon nanotubes are described and analyzed.

2. Methods for the production and modification of carbon nanotubes

2.1 Thermal sputtering

The most widespread method for carbon nanotube production is based on the thermal sputtering of a graphite electrode in an arc discharge plasma burning in an He atmosphere [4]. This method, which is also the basis for the most effective fullerene production technology [2, 3], permits the production of nanotubes in a quantity sufficient for a detailed study of their physical and chemical properties. In an arc dc discharge with graphite electrodes at a voltage of 15 – 25 V and current

of several tens of A, an interelectrode gap of several mm and an He pressure of several hundred Torr, the intense thermal sputtering of the anode material takes place. The deposit containing also some fullerenes among graphite particles covers the cooled walls of a discharge chamber as well as the cathode surface which is somewhat cooler than the anode surface. Observing this cathode deposit with the aid of a microscope Iijima [4] found that it contains elongated cylindrical tubes over a micron in length and several nm in diameter, the surface of which consists of graphite layers. The tubes are ended with cupola-like caps, the structure of which, like fullerene molecules, includes pentagons along with regular hexagons. The tubes are characterized by varied chirality, i.e. the orientation angle of the graphite plane relative to the axis of the tube.

In the conditions of the experiment [4], the content of nanotubes in a cathode deposit did not exceed several percent. Since nanotubes, like other carbon particles contained in a cathode deposit, are insoluble in organic solvents, their extraction in the pure state from a deposit presents serious technical problems. Further research efforts were directed to modification of the nanotube production procedure and enhancement of the yield. These studies showed that the conditions of burning in a graphite electrode arc, which are optimal for nanotube production, are somewhat different from those for fullerene production [32, 33]. The difference relates primarily to the buffer gas (He) pressure, which is close to 500 Torr in optimal conditions for nanotube production, whereas in the case of fullerene production this quantity is about 150 Torr. Besides that, an enhancement of nanotube yield is attainable by increasing the cathode diameter (over 10 mm).

The optimization of setups designed especially for this purpose has provided the possibility of producing nanotubes in gram quantities. The maximum nanotube yield in a cathode deposit exceeded 60%. One such setup described in detail in Ref. [34], is shown schematically in Fig. 1. In this setup special attention is paid to the problem of the effective cooling of electrodes. For this purpose copper gaskets are used for the electrodes, which are cooled through a multichannel water flow system. Besides that, our attention was engaged with the automated facility for keeping the interelectrode gap at a prefixed level of 1 – 2 mm. The indicated device promoted the enhanced stability of the arc discharge parameters, which proved to be the necessary condition for getting a high nanotube yield [35, 36]. The maximum nanotube yield is observed at as low as possible a current which ensures the stable burning of the arc. An occasional rise in the arc current even for several minutes transforms a quite good soot with a high nanotube content into a useless graphitized solid bulk. In the work [34], cylindrical electrodes 12.5 mm in diameter were used at an arc voltage ranging 17 – 20 V and current 110 – 130 A, and also electrodes 19 mm in diameter at a voltage 17 – 20 V and current 250 – 300 A. Up to 90% of the net mass of thermally decomposed anode material was managed to collect from the cathode surface in the process. As follows from the scanning electron microscope observations, multilayer nanotubes formed reach up to 40 μm in length. They grow normally to the cathode flat surface and form cylindrical bundles of about 50 μm in diameter. These bundles cover the cathode surface in a regular manner, forming a honeycomb-like structure, in which an interbundle space is filled with a mixture of randomly oriented nanoparticles containing nanotubes as well. Nanotubes in a bundle

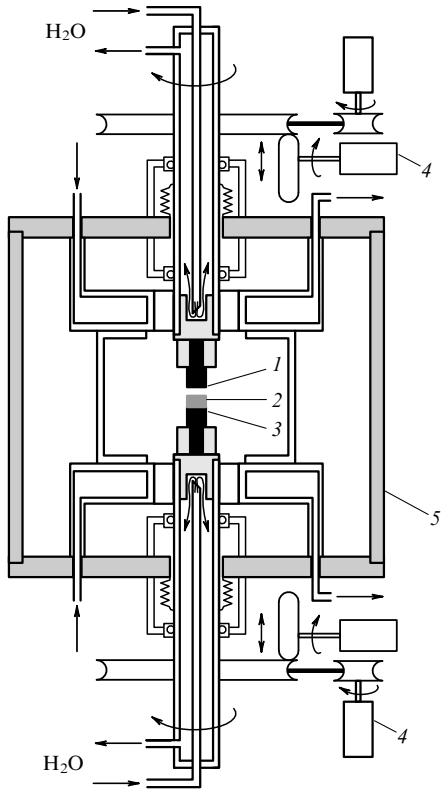

Figure 1. Schematic of an electric arc facility for producing nanotubes in gram amounts [34]: *1* — graphite anode; *2* — deposit containing nanotubes; *3* — graphite cathode; *4* — automated devices for keeping the interelectrode distance at the preset level; *5* — chamber wall. The directions of cooling water flows are shown by arrows.

tend to sinter. The hierarchy of the structure of nanotubes contained in soot was also noted in Ref. [36]. Nanotubes are observed to combine in small bundles, which together with nanoparticles form fibers up to 50 μm in diameter. In turn, the fibers form filaments of larger diameter which are visible to the naked eye. In optimal conditions the nanotube yield in a cathode soot reaches 60%.

High resolution electron microscope observations show the complicated spatial structure of a cathode deposit formed as a result of graphite-electrode arcing. Thus, in work [37] the soot deposited on the cathode surface formed a multishell cylindrical structure. A graphite cathode and anode of 2.5 and 1.25 cm in diameter, correspondingly, were used and the He pressure comprised 100 Torr, the discharge current ranged between 180 and 200 A and the voltage varied in the range 20 – 30 V. An inner gray rod was surrounded by a black ring, which in turn was embedded in a gray shell. The black ring contained a number of nanotubes of tens μm in length and various diameters. The intermediate region between the black ring and the outer shell contained carbon particles enclosed in graphite envelopes.

Besides the nanotubes in the cathode deposit a wide variety of nanoparticles shaped like polyhedron or other figures are also observed. The existence of such impurities quite significantly hinders the study of nanotubes using contemporary physical equipment. For this reason special methods were developed for the extraction of nanotubes from a cathode deposit. The most widespread method is based on the use of ultrasonic dispersal of a deposit placed for this

purpose in a suspension. Thus, in work [38], samples of a cathode deposit produced at an arc voltage of 18 V and an He pressure of 500 Torr, were sonicated in methanol which resulted in the separation of nanotubes from each other and from nanoparticles. The suspension produced after the addition of some water was treated in a centrifuge. Then the nanotubes floating in the suspension were washed in nitric acid, dried and oxidized for 5 min in an O_2/H_2 (1 : 4) stream at a temperature of 750 °C. This resulted in an additional purification of the material from nanoparticles. The material produced was comprised of multilayer nanotubes about 10 μm in length and 20 nm in diameter.

The physical reasons for the difference in the optimal conditions for generation of fullerenes and nanotubes in an electrical arc with graphite electrodes remain unclear. This is caused by the deficiency of experiments directed to the detailed exploration of the dependences of quantity and quality of nanotubes on the discharge parameters and other external conditions. Amongst a limited number of such works should be mentioned the recent publication [39], which contains the results of a detailed study of the dependences of both the nanotube yield in a cathode deposit and the thermal stability of this deposit in relation to the He pressure in the discharge. Soot containing nanotubes was produced in an arc discharge between graphite electrodes 6 mm in diameter at a voltage of 26 V, direct current of 60 A and an He pressure ranging between 80 and 700 Torr. The soot samples produced were studied through a high-resolution transmission electron microscope (TEM) as well as a differential thermal analyzer (DTA) and thermal gravimetrical analyzer (TGA). As follows from the DTA analysis, the thermal decomposition of the soot in air starts at a temperature of 670 °C and reaches a maximum intensity at 830 °C. This value is 300 – 400° above that for the C_{60}/C_{70} extract and close to 900 °C, which corresponds to the minimum temperature for the process of intense thermal decomposition of graphite. The thermal stability of a deposit rises with a rise in the He pressure during production. Table 1 shows the initial temperature T_0, at which a deposit weight loss is noted, the nanotube yield and the rate of cathode deposit growth vs. He pressure. The nanotube yield was determined through the visual analysis of TEM pictures. As is seen, the maximal rate of cathode deposit growth is reached at low He pressures, when the nanotube yield is minimum. Thus, it can be concluded that the decrease in the He pressure drastically changes the composition of a deposit in the direction of fullerene formation.

Table 1. Temperature T_0, at which a loss in the weight of a cathode deposit is detected, the nanotube yield in a deposit and rate of its mass growth as measured in work [39] at various magnitudes of He pressure.

He pressure, Torr	80	150	230	300	450	600	700
T_0, °C		706	714	723	753	774	800
Nanotube yield, %	8		15		20	30	40
Rate of the deposit massgrowth, mg min^{-1}	126	70	50	30	31	30	28

2.2 Production of open and single-layer nanotubes through oxidation

The nanotubes formed in an electric arc with graphite electrodes are mainly multiwalled with diameters ranging from one to several tens of nanometers. Besides that such nanotubes are distinguished by their chirality, which determines the diversity of their electronic structures and electrical characteristics. The size and chirality distributions of nanotubes depend drastically on the conditions of arc burning and are not reproducible from one experiment to another. This circumstance as well as the wide variety of sizes and shapes of nanotubes comprising a cathode deposit does not permit the consideration of this material as a substance with specific properties. This problem has been partially solved by processing the material under consideration with strong oxidizers. Such an approach was first demonstrated in Ref. [15] and has been further developed in Refs [9, 40, 41].

The methods for purifying and processing nanotubes through oxidizers are based on the difference in reactivity of carbon atoms belonging to an elongated graphite layer comprised of six-membered graphite rings, forming a cylindrical nanotube surface and those of the spheroidal surface of the nanotube cap, which also includes a number of five-membered graphite rings. The latter is much more reactive than the former. It follows, specifically, from the results of the direct measurements [42] presented in Fig. 2. In this experiment, a preweighted quantity of nanotubes produced by method [6] was heated in an open quartz vessel in the presence of air. A notable sample-weight loss was observed at $T > 700$ °C. At 850 °C, the sample fully disappeared over 15 min. As is seen from the comparison of the oxidation rates for fullerene C_{60} and nanotubes, fullerenes are oxidized at a temperature of about 200 °C lower than that for nanotubes. The activation barrier for the reaction of carbon nanotube oxidation in air is estimated as ~ 225 kJ mol^{-1}. As follows from the electron microscope observations, the oxidation process proceeds mainly near the end of a nanotube and primarily promotes the decomposition of its spheroidal cap. At 800 °C, about 20% of nanotubes are opened in 10 min. Besides cap oxidation, the stripping of the outer layers of nanotubes is also observed, which originates from the near tip region and takes place even in the case of not fully removed caps.

Carbon nanoparticles usually have an irregular polyhedral structure and much higher reactivity than nanotubes. This permits the use of a high-temperature carbon oxidation process for the transformation of a cathode deposit, containing a broad variety of nanoparticles besides multilayer

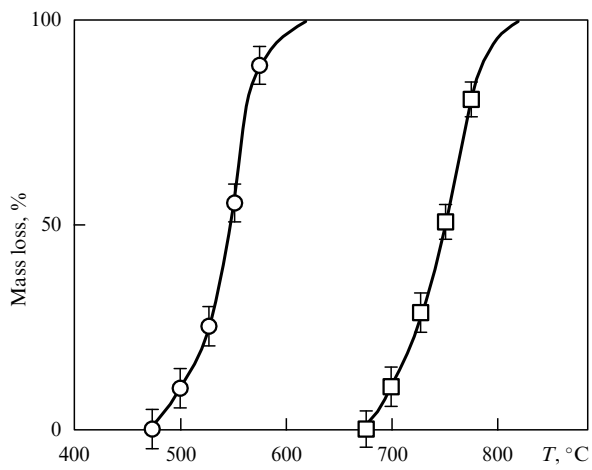

Figure 2. Temperature dependence of mass loss as a result of exposure to air for 5 minutes, measured for fullerene C_{60} (circles) and cathode deposit containing nanotubes (squares) [42].

nanotubes, into a material consisting mainly single-layer nanotubes. Such a possibility was shown for the first time in work [9], where the purification of nanotubes from nanoparticles through oxidation was performed at $T = 1000$ K. On the basis of direct observations it has been shown therewith that to remove all the nanoparticles it is necessary to oxidize more than 99% of the material.

For purifying and opening nanotubes as well as for stripping their outer layers not only oxygen of the air can be used, but also other gaseous oxidizers. Thus, in Ref. [40] for this purpose carbon dioxide (CO_2) was used quite successfully. The cathode deposit produced in an electric arc with graphite electrodes 8 mm in diameter and 15 cm in length at 30 V and 180 – 200 A dc, was conditioned with flowing CO_2 at $T = 850\,°C$ for 5 hours. It caused a 10% weight loss. As shown by electron microscope observations, the oxidation resulted in the opening of 5 – 10% of the nanotubes. There was also observed a partial decrease in the number of layers near the nanotube caps. The lower value of the oxidation rate of nanotube material in the presence of CO_2 in comparison with that for air oxygen permits a more effective control over the procedures of nanotube purification and modification to be exerted.

In purifying and opening nanotubes, as well as in stripping, liquid oxidizers can also be used and they can be more suitable in some cases. Thus, in work [41], a simple and effective method for selective opening of nanotubes using concentrated nitric acid as an oxidizer is developed. The cathode deposit was produced with the standard electric arc method. It contained about 25% multilayer nanotubes among the nanoparticles. Then 2 g of this material was washed in 45 ml concentrated nitric acid (68%) for 4.5 hours at a temperature of 240 °C. The insoluble substance after drying was sonically dispersed in chloroform and dried again in a vacuum. As shown by the tunnel electron microscope pictures, about 80% of the nanotubes were opened. Nitric acid processing for 24 hours resulted in the opening of about 90% of the nanotubes.

2.3 Thermal sputtering in an arc in the presence of a catalyst

Carbon nanotubes produced in an electric arc discharge are usually rather short (less 1 μm). This peculiarity as well as the relatively high cost of the material, caused by the low productivity of its synthesis, hinders the practical use of nanotubes. Most of the above-mentioned disadvantages of nanotubes have been overcome successfully by the further development of the arc discharge production technology intended for nanotubes with preselected characteristics using catalysts [10]. This approach has manifested itself quite well in the technology of producing hollow carbon fibers, which have extraordinary high mechanical characteristics and are widely applied [43 – 46]. Work [47] can be considered as a typical example of such an approach, where rare earth metals were used as a catalyst, specifically gadolinium and its oxides. In this case a hole 3.2 mm in diameter was drilled in an anode 8 mm in diameter and then filled with either powdered Gd_2O_3 or Gd. The content of Gd in the anode material amounted to 3 – 6 at. %. The graphite cathode was 12.7 mm in diameter. The arc burnt at the interelectrode gap of 3 – 6 mm, 85 A and an He pressure of 500 Torr in the case of Gd_2O_3 and 100 Torr in the case of pure Gd. The soot produced as a result of the anode-material thermal sputtering was ultrasonically dispersed in ethanol and was then coated on a copper grid covered with porous carbon for subsequent electron microscope observations. These observations show the formation of single-layer nanotubes < 75 nm in length, growing in bundles from amorphously structured particles Gd_xC_y. Some bundles also contain multilayer nanotubes. GdC_2 nanocrystals encapsulated in a graphite envelope were also observed. Similar results were obtained using Nd as a catalyst, whereas the use of La, Ce, Pr, Sm, Sc, and Er did not result in single-walled nanotubes.

The use of platinum group metals as catalysts proved to promote much more effective formation of elongated single-layer nanotubes. It was demonstrated in Ref. [48], where the dc discharge was performed at an He pressure between 100 and 600 Torr. A graphite rod 50 mm in length and 6 mm in diameter was used as an anode, from the outer edge of which was drilled a longitudinal hole 30 mm in length and 3.2 mm in diameter. The hole was filled with a mixture of powdered metal (Ru, Rh, Pd, Os, Ir, Pt) and graphite powder in the ratio 5 : 1 by mass. A pure graphite rod 13 mm in diameter was used as a cathode. The discharge current amounted to 70 A, the voltage was about 25 V, and the interelectrode gap was maintained by hand at the level of 1 – 2 mm. The products of the anode-material thermal sputtering were deposited on both the chamber walls and the plane and cylindrical cathode surfaces. Substances collected from the indicated places of the discharge chamber differed quite significantly from each other in their composition. The material taken from the edge cathode surface contained multilayer polyhedral nanocapsules from 20 to 200 nm in size filled with metal. As followed from the transmission electron microscope pictures, these nanocapsules consisted of up to 30 graphite layers, separated by 0.34 nm. As a rule, a crystal-structure metal cluster does not fully fill a capsule, so some cavity remained inside. The material taken from the inner surface of the discharge chamber contained spherical metal particles 10 – 30 nm in diameter in the case of Ru, Rh, Pd, and Pt and 5 – 10 nm in the case of Os and Ir, incorporated in the amorphous carbon structure. The material collected from the lateral cylindrical cathode surface contained metal particles from 3 to 10 nm in size, incorporated into single-walled or multi-walled carbon globules of complicated disordered structure. The formation of single-layer nanotubes from 10 to 200 nm in length and from 1.3 to 1.7 nm in diameter was observed under the catalytic action of Rh, Pd, and Pt. From some metal particles (specifically in the case of Rh) grew several tens of single-layer nanotubes, which resulted in the formation of sea-urchin-like structure. It was stated that the location of a single-walled nanotube is determined by the sort of metal used as a catalyst. Thus, in the case of Rh the maximum yield of single-walled nanotubes was stated for the material collected from the lateral cylindrical cathode surface, while the material taken from the edge surface also contained a small quantity. The inner surface of the chamber contained practically no single-walled nanotubes. The number of single-walled nanotubes formed in the presence of Pt and Pd was much less than in the case of Rh. In the case of Pt, nanotubes were observed on both the edge and lateral surfaces of the cylindrical cathode, while in the case of Pd they were found only on the cylindrical cathode surface and on the chamber walls.

The list of metals and other elements, which are effectively used as catalysts in the electric arc synthesis of carbon nanotubes, is quite long. This list also includes, apart from the elements mentioned above, Mn [49], Co [50 – 52], Fe [52 –

54], Ni [51, 52], Sc [55, 56], La [56 – 60], V [61, 62], Ce [63], Gd [64], Zr [57], Y [65, 66], and Ti [60, 61]. The presence of catalysts results in a considerable widening of the sorts of particles observed in a cathode deposit. In addition to nanotubes there were also found metal and metal-carbon compound (carbides) particles enclosed into a single-layer or multilayer graphite shell.

The parameters of nanotubes, nanoparticle content, shape and size of shells as well as the chemical composition and crystal structure of the material enclosed are determined by both the sort of a metal, used as a catalyst, and arc discharge parameters. Thus, the iron group metals used as catalysts promote the generation of single-layer nanotubes [52]. It is noted that while multilayer nanotubes grow usually out of the cathode surface, single-layer nanotubes therewith form in the gas phase. In work [52], single-layer nanotubes were produced under gas discharge conditions close to those optimal for the fullerene production, using Fe as a catalyst. The electrodes are situated vertically in the centre of a camera. The upper electrode 10 mm in diameter is used as an anode. The cathode 20 mm in diameter is supplied with a small dip in which a piece of iron is put. The chamber is filled with the mixture of 10 Torr methane and 40 Torr Ar. The arc burns at a voltage of 20 V and 200 A current. Vaporization of iron during the arc burning results in the generation of iron carbide particles, which condense over the cathode surface. The nanotube formation is observed only in the presence of Fe, Ar and CH_4 simultaneously. Unlike the well-known technology for catalytic production of carbon fibers using Fe as a catalyst [67], where iron particles are found at the end of growing threads and obviously promote their growth, in this case such particles are absent at the end of nanotubes. Probably, the atomic size particles stimulate the single-layer nanotube formation, acting as heterogeneous catalysts in the vapor phase. The samples for observation were prepared from the acetone suspension. As a rule, single-layer nanotubes observed in a deposit, are bound in bundles, whereas single nanotubes were also noted. The nanotube diameter ranges from 0.75 to 13 nm, and the maximum length reaches 700 nm. Figure 3 shows the histogram of nanotube diameters, obtained on the basis of observing 60 nanotubes. As is illustrated, the single-layer nanotube diameter distribution function extends from 0.7 to 1.6 nm and has the maxima at 0.84 and 1.05 nm. The similar results were obtained using Co as a catalyst [51], which also promotes the preferential formation of single-walled nanotubes.

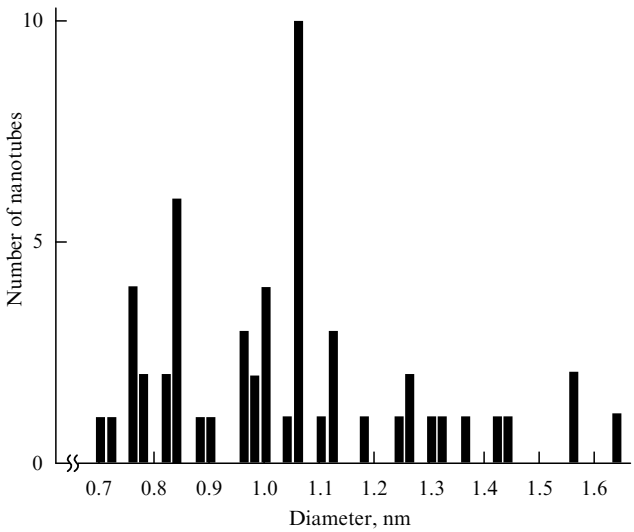

Figure 3. The histogram of diameters of single-layer nanotubes produced in an electric arc in the presence of iron catalyst [52].

The highest efficiency in relation to single-walled nanotube generation is reached by using mixed catalysts including two iron group metals [68]. In the work cited, the graphite rod cathode 9 mm in diameter was used as an upper electrode. In the centre of the anode 6 mm in diameter a hole of diameter 3 mm was drilled, filled with the mixture of two powdered metals in the wt. ratio 1 : 1. Argon was used as a buffer gas at a pressure of 550 Torr. The arc burnt at a voltage of 27 V and 75 A current. Filling the anode hole with Fe/Ni, Co/Ni and Co powders resulted in the formation of a web-like material containing mainly single-walled nanotubes over the near cathode area bordering the maximum electric-field strength region. The samples for electron microscope observations were prepared through the ultrasonic dispersion of a soot or a web-like material in benzene for 5 min. The copper grid was immersed into the suspension and then dried. The bundles were observed which comprised of 5 – 15 single-walled nanotubes ranging from 0.9 to 3.1 nm in diameter and over 5 μm in length. Unlike multiwalled nanotubes having mainly regular cylindrical shape, the single-walled nanotubes are usually highly bent, suggesting that they are flexible. The distribution function of single-walled nanotubes over a diameter, as obtained via processing the measured data for 70 nanotubes, has a sharp maximum at 1.7 nm. This distribution function rather weakly depends on the sort of the catalyst employed. It is significant that the single-layer nanotube content for mixed catalysts considerably exceeds that in the case of using only Fe, Ni or Co as a catalyst. This testifies that the metals act as a real catalyst rather than the heterogeneous centres of nucleation.

2.4 Laser sputtering

Carbon nanotubes as well as fullerenes are produced through thermal sputtering of a graphite. For this purpose some other methods for energy concentration on a graphite surface are also used quite effectively along with the gas discharge heating. The most convenient way for that is the laser irradiation of a graphite surface. Thus, the pulsed radiation of an Nd glass laser was used in work [69] as a source of the highly concentrated energy. A graphite rod (target) 1.25 cm in diameter was placed inside the quartz tube 2.5 cm in diameter and 50 cm in length, which in turn was enclosed in an oven. The target was blown with Ar at 500 Torr pressure and irradiated with pulses of the second harmonic of the Nd laser emission ($\lambda = 0.532$ μm) which were 10 ns in duration, 250 mJ in energy and 10 c^{-1} in repetition frequency. The diameter of a laser spot on the target accounted for 3 or 6 mm. Soot samples were taken from the water-cooled collector situated in the down-stream end of the tube, and also from the quartz tube walls and from the undersurface of the graphite rod. These samples contained multilayer nanotubes up to 300 nm in length with the number of layers ranging between 4 and 24. Single-layer nanotubes were not found in a deposit. As the oven temperature decreased, the quality of nanotubes reduced from defectless level at 1200 °C to defect-rich level at 900 °C. At 200 °C, nanotubes were absent at all. The similar temperature dependence of the nanotube yield takes place in the fullerene synthesis via laser vaporization. Authors of Ref. [69] suppose that nanotubes grow in the gas phase.

In the nanotube synthesis through the thermal action of the laser irradiation, the use of metal catalysts gives rise to the same qualitative effect as in the case of the electric arc synthesis considered above. The nanotube content in a soot is drastically increased and their quality is also improved significantly. Instead of multilayer nanotubes, which are distinguished by a substantial spread in diameters, the single-layer tubes are mainly formed in the process, the diameter of which ranges within relatively narrow limits.

Work [70] can be considered as quite demonstrative in this relation, which is in essence a continuation of work [65] cited above. Here, the above-described experimental chamber was also used, placed into the oven and arranged for the irradiation of a graphite target with laser pulses. However, mixtures of graphite and a small additive of a metal powder were used as irradiated samples. These samples were prepared in three stages. In the first stage, a paste formed through the mixing of a high-purity metal or its oxide with a carbon cement, filled a mold 1.25 cm in diameter. Then the mold was placed under a hydraulic press and held at a temperature of 120 °C and a constant elevated pressure for 4 – 5 h. The rod sintered in such a way was cured in flowing Ar at 810 °C for 8 h. The targets produced were heated up to 1200 °C in flowing Ar for 12 h. Besides, before each new experiment with the same target it was kept in flowing Ar at 1200 °C during 2 h. The following metal concentrations were used (at. %): Co (1.0); Cu (0.6); Nb (0.6); Ni (0.6); Pt (0.2); Co/Ni (0.6/0.6); Co/Pt (0.6/0.2); Co/Cu (0.6/0.5), and Ni/Pt (0.6/0.2). The second harmonic radiation ($\lambda = 0.532$ μm) of a pulsed Nd laser with an energy of 300 mJ/pulse was focused onto a metal-graphite composite surface in the form of a spot 6 – 7 mm in diameter. The target was situated in a chamber through which the Ar flux flowed at a pressure of 500 Torr. The chamber was enclosed in an oven, whose temperature could reach 1200 °C. A soot formed through laser thermal sputtering of the target, was removed with Ar flux from the heated area and then deposited onto a water-cooled copper collector. The soot samples were prepared for the electron microscope observations through sonication in methanol for 1 h. Single-layer nanotubes near 1 nm in diameter were also observed in the soot in addition to polyhedral nanoparticles, the yield of which increased with a rise in the oven temperature. In the case of a single metal used as a catalyst, the maximum yield of nanotubes is observed for Ni, followed by Co. The use of Pt results in a rather low yield, whereas the employment of Cu or Nb prevents the producing of nanotubes at all. In the case of bimetallic catalysts the maximum yield (about 15% of total carbon evaporated, which is 10 – 100 times as much as in the case of monometals) is observed for the Co/Ni and Co/Pt mixtures, which are followed by the Co/Cu and Ni/Pt mixtures providing a rather low single-walled nanotube yield. In a certain case the use of the Co/Ni mixture resulted in a 50% nanotube yield. A high quality of nanotubes synthesized is noted; they are free of outgrowths which are inherent to electric arc products.

High potentialities of laser graphite vaporization method, as applied to selective production of nanotubes with preset characteristics, were demonstrated in recent experiments [11, 71], which are based on the sequential irradiation of a nickel-doped graphite target with two laser beams of different wavelengths relevant to a visible range. This resulted in a predominant (up to 90% yield) formation of single-walled nanotubes of a certain diameter (1.38 nm) correlating with a given chirality (10,10). In a recent work [72] it was found that the predominant formation of single-layer (10,10) nanotubes can be also reached in a graphite-electrode arc discharge plasma using the powdered Ni + Y mixture as a catalyst.

2.5 Electrolytic synthesis

Physical conditions promoting the nanotube generation are of a great variety. In particular, the effective nanotube generation is observed not only in conditions pertinent to a near-surface low-temperature plasma, which is formed as a result of an electric arc or laser vaporization of a graphite target, but also in electrolysis conditions, where all substances involved in the process are in a condensed state. The electrolytic synthesis of nanotubes was first made in work [14]. A graphite cube 5 × 5 × 5 cm in size was used as an anode, in which a hole 2.5 cm in diameter and 3 cm in depth was drilled, filled with 1 g of LiCl salt. The melted salt heated up to a temperature of 600 °C was served as an electrolyte. The graphite cathode 3 mm in diameter was immersed into the melt. Passing the current of 30 A through the electrolyte for 1 min resulted in the formation of nanotubes and other carbon nanoparticles on the cathode surface, which were observed using an electron microscope.

The result of further modification of the facility for electrolytic nanotube synthesis is shown schematically in Fig. 4 [12, 13]. The cylindrical graphite rod 4 cm in diameter

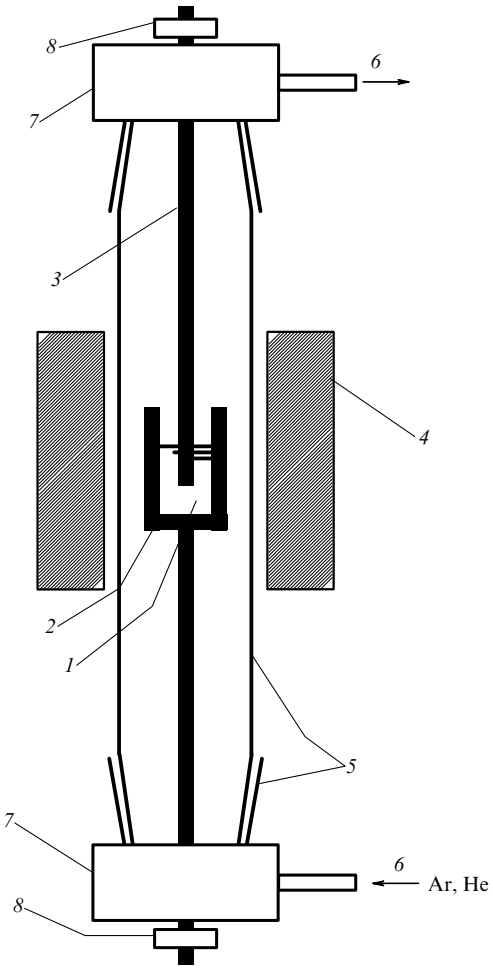

Figure 4. Schematic of the experimental setup for electrolytic synthesis of nanotubes [12, 13]: *1* — liquid electrolyte; *2* — graphite anode with a hole; *3* — graphite cathode; *4* — an oven; *5* — quartz tube; *6* — tubes for flowing gas; *7* — copper flanges; *8* — sealing rings.

and 10 cm in length was used as an anode, in the centre of which a cylindrical hole 3 cm in diameter and 7 cm in depth was drilled. Graphite rods 3 mm in diameter, inserted into dry LiCl in a depth of 1 – 3 cm were used as a cathode. The chamber was filled with Ar at a pressure up to 500 Torr. The crucible was heated up to a melting point of LiCl (604 °C). The electrolysis was performed during 4 min at currents of 1, 3, 5, 10, 20 and 50 A, a voltage up to 20 V and the depth of cathode immersion into electrolyte ranged from a fraction of a centimetre to 4 cm. This procedure provided 30 – 80 mg of a carbon material, which was treated further during 4 hours in a mixture of toluene and water. A dry residue was ultrasonically dispersed in acetone for 20 min. Afterwards samples of the suspension were placed with a dropper onto a copper-graphite grid 3 mm in diameter of an electron microscope and then dried. Some of the pictures obtained are presented in Fig. 5. It is found that the generation of nanostructures proceeds on the cathode, because they were observed using not only graphite, but also steel crucibles. Encapsulated nanoparticles, onion-like structures and carbon nanotubes of various morphology were found between the electrolysis products. The spiral and rolled structures engaged the researchers' attention. When using LiBr instead of LiCl as an electrolyte the qualitatively similar results were achieved. Adoption of LiI, having lower melting point, did not result in the appearance of a graphite nanomaterial. As evidenced from the analysis, the content of nanotubes in the soot reached 20 – 30%. In the initial stage of electrolysis (first minute) polyhedral particles encapsulated in graphite envelopes are mainly formed, while at higher energy inputs (between 3rd and 4th minutes) the nanotubes and threads appear. The relative yield of nanotubes and encapsulated particles increases with reduction in the current and cathode immersion depth. The current optimal for nanotube formation lies in the range between 3 and 5 A. At higher currents (10 – 30 A) the encapsulated particles and an amorphous carbon are mainly formed, whereas at lower currents (~ 1 A) an amorphous carbon is formed only. The nanotubes produced involve a number of layers with the interlayer spacing of 0.34 nm. The relative yield of various structures depended on specific conditions. In typical circumstances the voltage is equal to 3 – 4 V, the current is ~ 3 A, and the cathode immersion depth is 2 cm. The quantity of a material produced is roughly proportional to the electrolysis current.

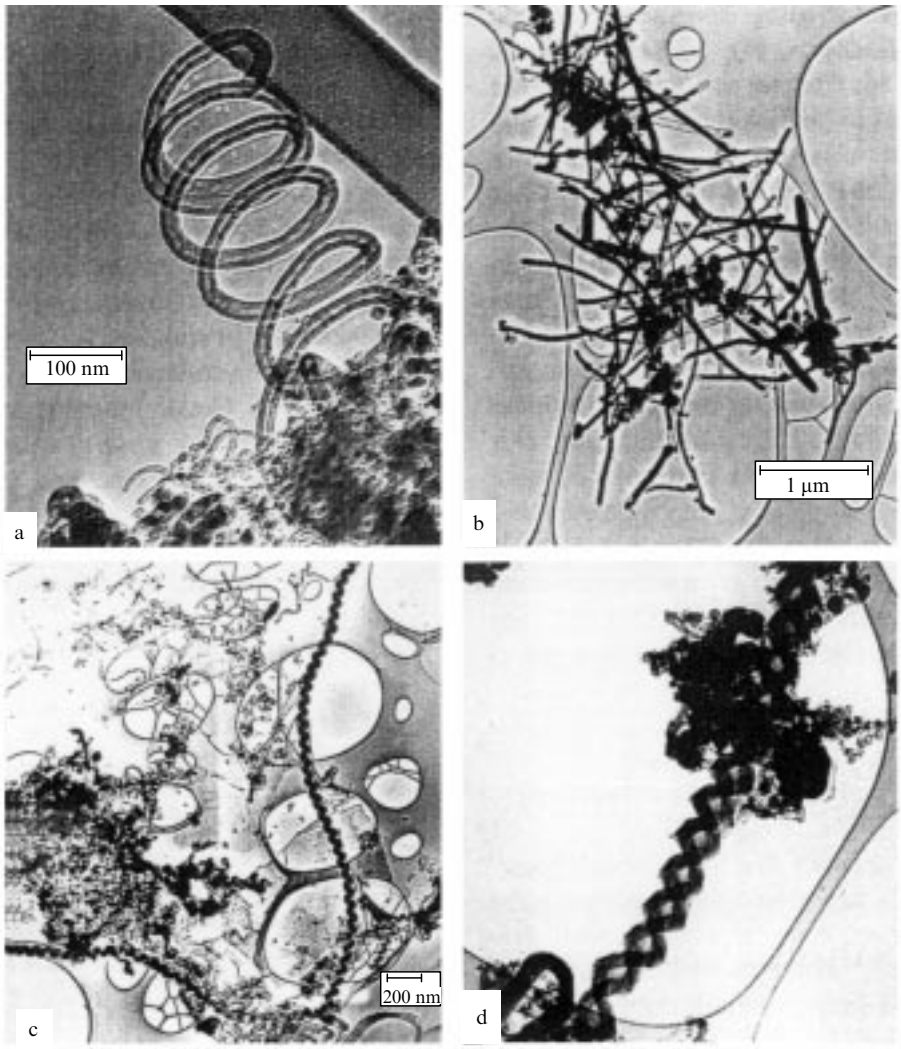

Figure 5. Electron microscope photographs of carbon structures formed under electrolytic decomposition of the graphite cathode [13]: (a) the electrolysis current is 3 A, depth of the cathode immersion in the melt is 1 – 3 cm; (b) the current is 3 A, depth of the cathode immersion in the melt is 0.5 ± 0.2 cm; (c) the sample containing a nanotube of the spiral structure; (d) double-spiral structure of the nanotube.

It should be noted that because the temperature in the region of the nanotube synthesis (900 K) is much less than that of the graphite layer decomposition, the mechanism of the nanotube growth cannot include the single-atom condensation, which was supposed earlier in explaining the mechanism of the nanotube synthesis in an electric arc discharge.

2.6 Catalytic cracking of acetylene

One more effective method of generating carbon nanotubes is based on the process of thermal decomposition (cracking) of the acetylene in the presence of catalysts [74, 75]. This method, permitting to generate the nanotubes in a wide range of changing their physical characteristics, was gathering force in the set of works [76–81]. Transition metals Fe, Ni, Cu and Co of several nanometers in size were used in these works as catalysts. The procedure of nanotube generation has been optimized and described in detail in Ref. [77]. A ceramic cup containing 20–50 mg of a catalyst is placed into a quartz tube 60 cm in length and 4 mm in inner diameter. Acetylene C_2H_2 admixed to a nitrogen in the content of 2.5–10% is pumped through the tube heated up to $T = 773-1073$ K for several hours at the rate of 0.15–0.59 mol (C_2H_2) per hour. To prepare the catalyst, amorphous carbon flakes of natural origin are injected into metal salt solvents (Fe or Co oxalate or Ni or Cu acetate), which results in the generation of metal particles surrounded by graphite shells. The weight content of a metal ranges between 0.5 and 10%. Besides that, a silica gel 9 μm in pore diameter is inserted in the water solution of Fe or Co nitrates for production of a catalyst on the base of SiO_2. The weight content of a metal in the material produced accounts for 2.5%. All catalytic samples are dried for several hours at $T = 403$ K, and then calcinated for 2 h at 773 K and reduced in a flow of N_2 with a 10% admixture of H_2 at $T = 773$ K during 8 h.

The catalytic acetylene cracking is performed at 700 °C. The above-described procedure gave rise to 4 sorts of carbon structures: a shell of an amorphous carbon on a catalyst surface; filaments of an amorphous carbon; metal particles enclosed in a graphite multishell envelope, and, finally, tubes consisted of graphite layers and typically coated on the outside with an amorphous carbon. The least value of the inner diameter of filaments is 10 nm. The outer diameter of filaments free of an amorphous carbon coating ranged between 25 and 30 nm, whereas for coated filaments it reached 130 nm. The length of nanotubes varies from several portions to several tens of a micrometer. The yield of nanotubes in a sample depends on the sort of catalyst and in the case of Co it is much higher than for iron. In the case of Ni the filaments have an amorphous structure. For copper catalyst all carbon precipitates in an amorphous form. The tubes produced with a catalyst on the base of a silica gel are thinner than that for catalyst on the base of a graphite. Likewise graphite-based catalysts, a silica gel doped with Co results in higher nanotube yield than with Fe. Using the silica gel doped with Co was found capable of producing spiral nanotubes in parallel with conventional ones. It was revealed that the treatment of a catalyst after nanotube synthesis with a mixture of nitrogen and hydrogen at 873 K causes the gasification of an amorphous carbon and cleaning of the nanotube surface from the latter. This procedure is akin to the previously described oxidation method used for opening and layer-to-layer peeling of multilayer nanotubes [9, 15, 40–42].

The distinctive feature of the above-described method for nanotube synthesis is a wide diversity of modifications and a high quality of samples produced. Thus, in work [76], hollow multilayer nanotubes 3–7 nm in inner diameter, 15–20 nm in outer diameter and up to 30 μm in length, which involved 8–10 graphite layers were observed along with single-layer and multilayer nanotubes of different diameters. Some quantity (about 10%) of the spiral nanotubes of different radii and pitches was found along with straight tubes, which were typically observed in pairs. The smallest spiral observed is about 8 nm in radius. Surfaces of the nanotubes produced are usually free from an amorphous carbon coating, which is caused by a prolonged treatment of nanotubes with heated gases (N_2 and H_2).

2.7 Other methods for the nanotube production

Like the fullerenes, the carbon nanotubes are effectively formed within a wide range of conditions. Therefore, various methods and approaches are used in their synthesis. Besides those described above, the work [103] is also worth mentioning as it demonstrates a possibility of producing fullerenes and nanotubes in flames of acetylene, benzene or ethylene, premixed with oxygen and a buffer gas. The gas pressure therewith varied in the range 20–97 Torr; the atomic ratio C/O accounted for 1.06 in the case of C_2H_2, 0.86–1.0 (C_6H_6) or 1.07 (C_2H_6); the speed of gas flow at the burner outlet ranged from 25 to 50 cm s^{-1}, and a maximum flame temperature was near 2000 K. Soot samples were extracted from the flame using a water-cooled suction probe and also from the water-cooled walls of a burning chamber. Afterwards they were ultrasonically dispersed in toluene. As evidenced by high-resolution electron microscope observations, the samples contained about 10% multilayer nanotubes 2–15 nm in size and 0.34–0.36 nm in interlayer spacing. Some particles represented cylindrical nanotubes ended with two hemispheres.

One more procedure aimed at the carbon nanotube production has been proposed and realized in a previous work [105] and received further development. This method received the name quasi-free vapor condensation. Carbon vapor generated as a result of the resistive heating of a graphite tape, is condensed in a vacuum $\sim 10^{-8}$ Torr on a highly ordered pyrolytic graphite substrate cooled down to a temperature of 30 °C. The electron microscope observations show that the films 2–6 nm in thickness contain carbon tubes 1–7 nm in diameter and up to 200 nm in length. The most of the tubes are ended with a hemispherical cap. The nanotube content in a deposit exceeds 50%. The interlayer spacing in multilayer tubes measures 0.34 nm. The tubes are arranged on a substrate practically horizontally.

3. Nanotube structure

3.1 Chirality

An ideal nanotube represents a graphite plane scrolled into a cylinder, i.e. the surface consisting of regular hexagons in whose vertices the carbon atoms are placed. The result of scrolling depends on the orientation angle of a graphite plane in relation to the nanotube axis. This orientation angle determines the chirality of a nanotube, which governs in particular its electrical properties. The chirality of nanotubes is illustrated in Fig. 6 [21, 54], where a part of a graphite plane is depicted and possible directions for its scrolling are marked.

The nanotube chirality is denoted by the pair of symbols (m, n) showing the coordinates of the hexagon on the graphite

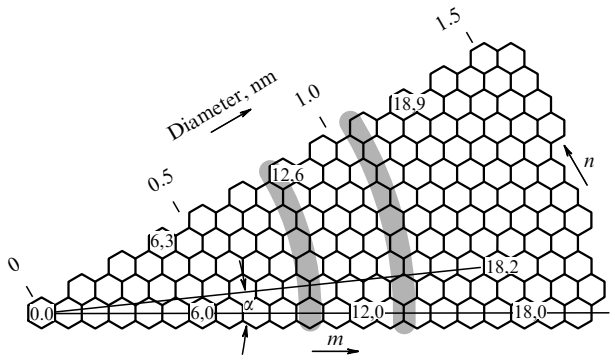

Figure 6. The illustration of the nanotube chirality after Refs [21, 54]. A part of the graphite surface is given, the scrolling of which into a cylinder provides the formation of a single-layer nanotube.

plane, which has to be superimposed on the origin hexagon as the result of scrolling. Some of these hexagons are shown in the figure along with related labelling. Another way of chirality labelling consists in indication of the angle α between the direction of a nanotube scrolling and that of the common side of two adjacent hexagons. Amongst different possible directions of nanotube scrolling are distinguished those, for which bringing of the hexagon (m, n) into coincidence with the origin requires no distortion in its structure. These directions correspond to the angles $\alpha = 0$ (armchair configuration) and $\alpha = 30°$ (zigzag configuration). Such configurations are labelled by the chirality indices $(m, 0)$ and $(2n, n)$, respectively.

The chirality indices of a single-layer nanotube (m, n) uniquely determine its diameter D. This relation is obvious and has the following form:

$$D = \sqrt{m^2 + n^2 - mn}\,\frac{\sqrt{3}\,d_0}{\pi}\,, \tag{1}$$

where $d_0 = 0.142$ nm is the distance between neighbouring carbon atoms in the graphite plane. The angle α is expressed through the chirality indices (m, n) by the relation

$$\alpha = \tan^{-1}\frac{\sqrt{3}\,n}{2m - n}\,. \tag{2}$$

The resolution of modern electron microscopes is insufficient for direct discrimination of nanotubes with different chiralities, therefore the main method for determination of this parameter consists in measuring their diameter.

3.2 Single-layer nanotubes

An idealized model of a single-layer nanotube is depicted in Fig. 7 [82]. Such a tube does not form any seams on scrolling and is ended with hemispherical caps containing six regular pentagons along with hexagons. The presence of pentagons at the tube ends permits the nanotubes to be considered as a limiting case of the fullerene molecule, whose longitudinal axis length considerably exceeds its diameter.

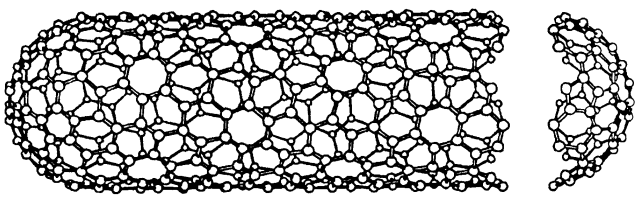

Figure 7. The ideal model of a single-layer nanotube [82].

The structure of single-layer nanotubes examined experimentally is distinct in many respects from the idealized picture presented above. This distinction primarily concerns the caps of a nanotube, the shape of which, as it follows from observations, is far from the ideal hemisphere.

Amongst single-layer nanotubes of particular interest are so called armchair nanotubes or nanotubes (10,10) in chirality. In such a nanotube, two of C – C bonds incorporated into a six-member ring, are aligned in parallel with the longitudinal axis of a tube. As follows from the calculations [17 – 24], nanotubes with such a structure should have purely metallic conductivity. Furthermore, thermodynamic calculations [71] show the enhanced stability of such tubes. So they have to dominate over tubes of alternative chirality in the conditions favourable for generation of single-layer tubes. Until the present time such ideal conditions seemed to be unattainable. However, the theoretical conclusions have found an experimental verification in the first-rate work [71], where on irradiating a graphite surface with two laser pulses in the presence of Ni – Co catalyst the metal-conductive nanotubes 1.38 nm in diameter and some hundreds μm in length were synthesized. As follows from electron microscope observations and X-ray diffraction measurements, nanotubes of predominant chirality (10,10) form bundles 5 – 20 μm in diameter, scrolled into mats and tangled in an odd manner. What is more, NMR-spectroscopy observations confirmed by direct measurements of nanotube conductivity, point to the metallic character of electrical transport in these samples.

Direct measurements of the chirality of nanotubes produced in Ref. [71] were performed in one of the subsequent work of the same group [107]. For this purpose the authors used a diffraction electron microscope with an extremely small cross section (about 0.7 nm) of an electron beam, which was quickly scanned over the area 10 – 20 nm in diameter, filled with a nanotube bundle. On the base of a diffraction pattern obtained in such a manner there are conclusions to be made about the structure of nanotubes incorporated to a bundle. Neither more no less than 35 bundles ranging from 3 to 30 nm in diameter were examined. All but two bundles were consisted of nanotubes of chirality close to (10, 10). The detailed analysis shows that 44% nanotubes have chirality (10,10), 30% (11,9) and 20% (12,8).

3.3 Capillarity and nanotube filling

Shortly after discovery of the carbon nanotubes the attention of researchers was engaged to the problem centred around the possibility of nanotube filling with various substances. This problem has not only purely scientific but also important applied significance, because a nanotube filled with a conductive, semiconductive or superconducting material may be considered as the most tiny element of microelectronics familiar to us today. The basic scientific interest to this problem is created via a possibility to obtain an experimentally justified answer to the question: at what minimum nanotube size the capillary phenomena hold their peculiarities inherent to macroscopic objects? It is conceivable that this subject was first considered in work [83], where the problem of the molecule HF drawing inside the nanotube under the action of the polarization forces was analyzed theoretically. In doing so it was concluded that the capillary phenomena resulting in drawing in liquids, wetting the inner

surface of a capillary, retained their nature on transferring to tubes of nanometer diameter.

Capillary phenomena in carbon nanotubes were first established experimentally in work [15], where the effect of capillary drawing in molten lead inside nanotubes was observed. In this experiment the electric arc at a voltage of 30 V and 180–200 A current designed for nanotube production, was ignited between the electrodes 0.8 cm in diameter and 15 cm in length. As a result of thermal decomposition of the anode surface, a material forming a layer 3–4 cm in height was deposited on the cathode surface. This substance was extracted from the chamber and conditioned at $T = 850°C$ for 5 hours under flowing carbon dioxide. This procedure resulted in a weight loss of about 10% and promoted the removal of amorphous graphite particles from the sample surface and opening of nanotubes contained in a deposit. The interior of a deposit containing nanotubes was introduced into ethanol and ultrasonicated. The product of oxidation dispersed in chloroform was then supported on a carbon tape with holes designed for making transmission electron microscope observations. The latter showed that untreated tubes possessed the seamless structure, regular shape of caps with a diameter ranging between 0.8 and 10 nm. The oxidation resulted in a damage of caps for about 10% nanotubes and partial stripping of layers around caps. The sample containing nanotubes to be examined was filled in a vacuum with molten lead droplets produced by irradiating a metal surface with an electron beam. In this case the lead droplets ranging from 1 to 15 nm in size were observed on the outer surfaces of nanotubes. The latter were annealed in an air at $T = 400\,°C$ (higher than the melting point for lead) for 30 minutes. As evidenced by the electron microscope observations, a portion of nanotubes was found after annealing to be filled with a solid material. A similar effect of the tube filling was observed on irradiating tube caps, opened as a result of annealing, with a powerful electron beam. A sufficiently strong irradiation gave rise to the melting of a material located near the open end of a tube and its penetration inside a tube. The occurrence of lead inside tubes is evidenced through the X-ray diffraction and electron loss spectroscopy methods. The thinnest lead wire is 1.5 nm in diameter. The observations showed that the portion of filled nanotubes did not exceed 1%.

The subsequent effort of researchers in the direction considered was mounted the detailed study of peculiarities of capillary phenomena in carbon nanotubes, which are exhibited on filling nanotubes with substances of various nature. Some results of such studies are represented in works [35, 36, 42, 84, 85]. These results point to the interconnection between the magnitude of the surface tension of a substance and a possibility of its capillary drawing inside a carbon nanotube. Some results are generalized in Table 2 [36], where the experimental data concerning the possibility of the capillary drawing of various liquid substances inside carbon nanotubes are correlated with the magnitude of their surface tension. As seen, the capillary properties of nanotubes show themselves only in relation to the materials having a rather low (less than 200 mN m^{-1}) magnitude of the surface tension in the liquid state. This conclusion is in agreement with a qualitative analysis of the phenomenon performed by Ebbesen [35, 36].

Analyzing experiments related to the investigation of the capillary phenomena in nanotubes, we should focus our attention on the role of oxygen, whose presence often determines experimental results. Thus, the experiments directed to nanotube filling with lead and bismuth in a vacuum have failed, whereas the similar experiments performed in the presence of an atmospheric air have resulted in the occurrence of the capillary effect. This observation is quite explicable from the viewpoint of the above-expounded consideration of the correlation between the capillary phenomena and the magnitude of the surface tension of the melt. The surface tension of molten lead and bismuth oxides is much superior to that for pure molten metals, therefore the presence of oxygen producing oxides promotes the occurrence of capillary phenomena.

Table 2. Wetting properties of nanotubes (the temperature is close to the melting point; the lead and bismuth oxides stoichiometry is uncertain) [36].

Substance	Surface tension, mN m^{-1}	Capillary effect
HNO_3	43	Yes
S	61	Yes
Cs	67	Yes
Rb	77	Yes
V_2O_3	80	Yes
Se	97	Yes
Lead oxides	(PbO ~ 132)	Yes
Bismuth oxides	(Bi_2O_3 ~ 200)	Yes
Te	190	No
Pb	470	No
Hg	490	No
Ga	710	No

As noted in work [85], for the manifestation of the capillary effect in relation to liquid metals with a high magnitude of the surface tension it is insufficient to use the standard procedure described above. In such a case it should be added with special contrivances. One method aimed to solve this problem is in applying an outer pressure which permit the pushing out force to be overcome.

Another way, being proposed and realized in Refs [86, 87], is based on the employment of solvents having low surface tension and for this reason capable to penetrate inside nanotubes due to capillary phenomenon. In so doing the authors used quite effectively as a solvent the concentrated nitric acid characterized by rather low magnitude of the surface tension (about 43 mN m^{-1}). The soot containing nanotubes was produced by an electric arc graphite vaporization. The productivity of the facility was about 15 g/h of cathode deposit containing up to 25% nanotubes along with carbon nanoparticles. 2 g of that deposit was inserted into 45 g of nitric acid 68% in concentration and was conditioned at a temperature of 240 °C for 4.5 hours. After drying an insoluble substance was ultrasonicated in chloroform and dried again in a vacuum. The tunnel electron microscope images of the resulting material show about 80% nanotubes to be opened. The treatment with the nitric acid for 24 hours resulted in the opening of about 90% nanotubes. For filling nanotubes with a metal dissolved in the nitric acid, a suspension containing 0.4 g of closed nanotubes and 20 g of nitric acid solution (involving 1 g of the hydrated nickel nitrate) was prepared. The suspension was conditioned at a temperature of 140 °C for 4.5 hours. After filtration and drying the sample was heated up to 450 °C with flowing He and annealed at the same temperature for 5 hours. As follows from the observations it promoted the opening of 80% nanotubes, 60–70% of which contained a nickel material. The similar material was also formed on the outer surfaces of nanotubes and nanoparticles.

The crystal structure of this material corresponds to NiO. Crystals of NiO located inside the nanotubes are 3 – 6 nm in diameter and up to 30 nm in length. They are usually situated rather far from the open ends of nanotubes. The treatment of closed nanotubes with uranil nitrate dissolved in nitric acid permitted the investigators to produce nanotubes filled with an uranium-bearing substance, which contained 70% of uranium oxide. The similar results were obtained for Fe and Co. The treatment of samples containing Ni, Co and Fe oxides with hydrogen at a temperature of 400 °C for 4 hours seemingly caused the reduction of metal crystals from oxides. The processing of nanotubes filled with uranium oxides with water solution of nitric acid resulted in dissolving of a main part of uranium-containing crystals and their escaping from nanotubes. In filling nanotubes the solutions of metals and their oxides in nitric acid were used. Here nitric acid plays a twofold part: to open nanotubes and to encourage the metal penetration inside. The low magnitude of the surface tension of nitric acid is used in the process, which in accordance with the considerations given above should wet the inner nanotube surface.

The most natural method for production of nanotubes filled with metals and their compounds is based on the technology of catalytic nanotube synthesis using metals as catalysts. In so doing the nanotubes are filled with metals and compounds in the process of synthesis, which permits the above-indicated limitations, related to the magnitude of the surface tension of molten metals, to be avoided. As a result of such an approach the multilayer nanotubes filled fully or partly with crystals of metals, their oxides or carbides are usually generated. The number of elements, which were managed to be inserted inside tubes in such a manner, is quite large; a reader can find the list of these elements in the preceding section (p. 000). Mention should be made of the considerable variety of crystal forms and chemical states for encapsulated metals. Thus, in work [53], where the iron group metals (Fe, Co, Ni) were used as a catalyst in the synthesis, not only crystal metal particles (bcc-Fe, fcc-Co, fcc-Ni), but also carbides X_3C (X is the metal atom) were found inside nanotubes.

The special attention should be paid to work [16], where carbon nanotubes filled with superconducting material TaC were produced. The success in this experiment has opened a perspective for using carbon nanotubes in the superconducting technology.

To produce encapsulated TaC crystals, the powdered Ta of purity 99.9% and finely ground graphite were mixed in the wt. ratio of ~ 0.6 and impressed into a hollow graphite rod 8 mm in length, 3 mm in inner diameter and 6 mm in outer diameter, used as an anode. An arc burnt in the He atmosphere at a pressure of 100 – 300 Torr, 30 V voltage, 30 A current and the interelectrode gap of 2 – 3 mm. The fixed cathode was 17 mm in diameter. The temperature of the end cathode surface was estimated as 1500 °C. Discharge burning resulted in the generation of a carbon deposit with an admixture of TaC particles on the cathode surface, which were found both on the surface and in the bulk of the deposit. For extraction of TaC particles incorporated into graphite shells, the deposit samples (100 mg) were inserted into 75% solution of sulfuric acid and conditioned at a temperature of 80 °C during two weeks. As a result of this procedure the nonencapsulated particles were fully dissolved in acid. The rest of the particles were repeatedly washed with a distilled water, dried and dispersed using ultrasonication in ethanol. Afterwards one-two drops of a suspension were placed with a dropper onto a carbon-coated copper grid for making the electron microscope observations. As follows from the observations, the cathode deposit contains a large quantity of TaC crystals encapsulated in nanotubes, and a bar handful of crystals encapsulated in elongated or compact polyhedrals. By contrast, a large quantity of particles enclosed in polyhedral cells and a small quantity of short nanotubes was found in a substance taken from the partly sputtered anode surface. In what follows an attention will be paid to particles extracted from the cathode deposit. TaC particles ranging from 2 to 20 nm in size with a maximum in the distribution function at 6 nm are usually enclosed in multishell nanotubes with interlayer spacing 0.3481 nm, which is 3.9% higher than for pure graphite. The structure of the encapsulated TaC was studied using the X-ray diffractometry. This structure is not different from the conventional crystal structure of TaC, which corresponds to that of the table salt NaCl with the lattice constant $a_0 = 0.4455$ nm. The superconducting transition was observed at $T = 10$ K through the magnetic susceptibility measurements. The distinctive feature of TaC is in its extraordinary high melting point (3985 °C), which is maximum among all carbides and is much over the melting point of the pyrolythic graphite (2500 – 3500 °C). This permits us to believe that a carbon nanotube enclosing a carbide thallium particle is formed as a result of the carbide crystallization.

One more interesting method for production of nanotubes filled with a metal was demonstrated in work [88], where gaseous iron compound $Fe(CO)_5$ was used as a metal-containing agent. A graphite electrode arc burnt in the mixture of He (50 mbar) and $Fe(CO)_5$ (50 – 200 mbar), which dissociated at high temperatures, releasing Fe. The interelectrode voltage accounted for 20 V, and the current covered 100 A. The soot produced in the gaseous phase as a result of the discharge burning was dispersed in the spirit and then suited on a copper grid for making the electron microscope observations. In a soot collected from the chamber walls the fullerenes were observed along with carbon nanoparticles containing particles of iron and iron carbides on the inside. The iron content was varied through the change in the temperature of the reservoir with liquid $Fe(CO)_5$, which determined a partial pressure of this gas. The chemical analysis of a soot taken from the chamber walls showed the iron concentration ranging from 1.8 to 12 wt. %. The soot contained iron nanoparticles, incorporated into a graphite envelope, and also a large amount of multilayer carbon nanotubes, partly filled with iron. The diameter of the nanotubes ranged between 20 and 65 nm, and their length reached 2.5 μm. The shape of the tubes was far from the linear one; they were filled with a metal only partly, but not over all their length. Nevertheless, the interlayer spacing was always equal to 0.34 nm. The metal enclosed in nanotubes had either monocrystal or polycrystal structure. In some cases there was present the included particles FeC and Fe_3C (cementite).

The most detailed study of peculiarities in filling carbon nanotubes with various metals is presented in the recent work [89], whose authors performed the experiments resulting in the encapsulation of 17 various metals inside nanotubes. The experimental setup was described in detail in a preceding work of the same authors [90]. Graphite rods 9 mm in diameter and 42 and 72 mm in length were used, correspondingly, as an anode and a cathode. The drilled hole in the anode 6 mm in diameter and 38 mm in depth was filled with a

mixture of graphite and metal powders. The arc burnt for 30 – 60 min at interelectrode separation of several mm, 100 – 110 A current, 20 – 30 V voltage and the He pressure of 450 Torr. The experimental data are given in Table 3. Two types of the nanotube filling with metals may be distinguished. The first one is observed in the case of Cr, Ni, Dy, Yb and Gd. In this case the nanotubes are uniformly filled lengthwise with a metal forming a wire of constant diameter, which is aligned strictly in parallel with the axis of a tube. These are real metal wires ranging from 100 nm to over 1 μm in length, surrounded with a graphite envelope. The second type of filling is observed in the case of Pd, Fe, Co and Ni. In this event the nanotubes are filled incompletely along their full length with a metal, which may be found as encapsulated particles located from place to place along the nanotube length and near its cap. The nanotubes nonuniformly filled with a metal over the length are variable in their diameter, while graphite layers remain to be aligned along the tube axis. In all cases but Co and Cu, where nanotubes are filled with a pure metal forming the face-centred crystal structure, a metal is incorporated into carbide. Thus, the carbides Fe_3C (cementite), Ni_3C and TiC have been identified.

Table 3. Experimental data related to nanotube filling with metals [89, 90].

Element	Ti	Cr	Fe	Co	Ni	Cu	Zn	Mo
Size of the metal grain, μm	10	5	1	2	10	40	10	10
Boiling point, K	3562	2945	3135	3201	3187	2836	1180	4912
Filling of nanotubes	–	+	+	+	–	–	–	
Unfilled shells	–	+	+	+	+	–	–	–
Length of the filled section of a tube, nm		3000	200	200	1000			
Number of holes	0	7	5	3	2	0	0	
Element	**Pb**	**Sn**	**Ta**	**W**	**Gd**	**Dy**	**Yb**	**Sm**
Size of the metal grain, μm	1	20	40	5	400	400	400	
Boiling point, K	3237	2876	5731	5828	3539	2835	1467	
Filling of nanotubes	–	+	+	+	+	–	–	+
Unfilled shells	–	+	+	+	+	–	–	+
Length of the filled section of a tube, nm	1000	3000	200	200	1200	600	200	10
Number of holes	2	0	0	0	7	5	1	9

As is seen from the experimental data presented in Table 3, the formation of metal nanowires inside carbon nanotubes does not depend on the boiling point of the metal. It follows that in the first stage of nanotube synthesis the temperature of an arc in the region of vaporization exceeds the boiling point for the metal and graphite. The observed correlation between the formation of nanowires and existence of unfilled electron shells in metal atoms shows that in the process of nanotube filling with metal ions the latter are found in the most stable oxidizing state. As is seen from the table, the more the number of vacancies in unfilled shells, the larger the length and higher the quality of nanowires. Thus, Cr and Gd are the best metals for nanowire production, having the maximum number of vacancies in unfilled electron shells and forming the longest wires.

Carbon nanotubes can be filled not only with liquid but also with gaseous substances. Such a possibility was demonstrated in the recently published work [91], where the results of experiments relating to single-layer nanotube filling with molecular hydrogen were presented. These results are of a great practical significance, because they open a possibility for solving the practically important problem of the safe storage of hydrogen, used as a fuel in ecologically pure car engines.

A soot containing single-layer nanotubes was synthesized in an electric arc with graphite electrodes doped with powdered cobalt. In this case the fibers several μm in length, consisted of 7 – 14 single-layer nanotubes (near 1.2 nm in diameter) bound into bundles, were obtained. Besides, there was also present Co nanoparticles ranging from 5 to 50 nm in size, incorporated into an amorphous carbon. The content of Co accounted for 20 wt. %. The samples of a soot containing single-layer nanotubes together with those of an activated charcoal used for comparison were placed into platinum foil packages equipped with holes promoting the gaseous diffusion. These samples were kept in hydrogen at a pressure of 300 Torr and a temperature of 273 K for 10 minutes, and in some cases 3 minutes more at the same pressure and a temperature of 133 K; afterwards they were cooled down to 90 K and pumped out. The H_2 content in samples was determined using the method of a temperature programmable desorption. As follows from measurements, the intensity of hydrogen desorption from the soot containing nanotubes is about 10 times greater (at the same temperature) than that for the activated charcoal. The activation energy for desorption is estimated as 19.6 kJ mol^{-1}.

3.4 The structure of multilayer nanotubes

Multilayer nanotubes are distinguished from single-layer ones by considerably more wide variety of shapes and configurations. The variety of structures reveals itself in both longitudinal and transverse directions. Possible versions of the transverse structure of multilayer nanotubes are shown in Fig. 8 [81]. The 'Russian dolls' structure (Fig. 8a) is a set of single-layer cylindrical tubes coaxially stacked one into another. The other modification of this structure, shown in Fig. 8b, is a set of coaxial prisms stacked one into another. Finally, the last of the structures presented (Fig. 8c) looks like a scroll. For all structures shown the magnitude of the interlayer spacing is typically close to 0.34 nm, which is

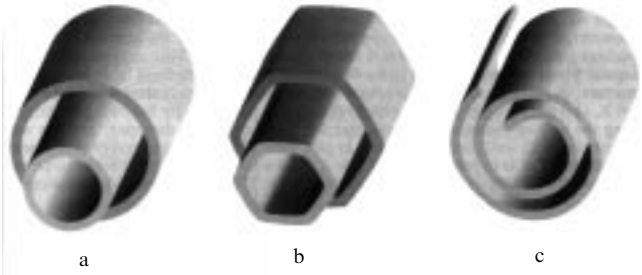

Figure 8. Models pertaining to transverse structures of multilayer nanotubes [81]: (a) 'Russian dolls'; (b) hexahedral prisms; (c) the scroll.

inherent to that of the crystal graphite. The realization of one or other type of the structure in the specific experiment depends on the nanotube synthesis conditions.

It should be noted that in spite of repeated attempts of researchers, any direct experimental data showing the domination of one or other structure of multilayer nanotubes synthesized in specific conditions, have not been obtained up to now. This is caused by insufficiently high resolution of the contemporary experimental apparatus (in particular, the electron microscopes and X-ray diffraction devices). Using the equipment mentioned permits the investigators to measure the interlayer spacing in a multilayer nanotube with a sufficient accuracy, but does not permit them to discriminate between the scroll and 'Russian dolls' structures.

The most convincing, in our opinion, experiment being indicative of the existence of both types of structures is described in the recent publications [93, 94]. In these works, a possibility was first shown for the intercalation of atoms K and molecules $FeCl_3$ inside carbon nanotube bundles to modify their electronic structure. It was found therewith that the possibility mentioned is largely dependent on the conditions of the nanotube production.

Multilayer nanotubes produced in two ways were used as a starting material: in a graphite-electrode arc discharge and through the chemical vapor deposition with iron or nickel particles as a catalyst (this method is described in detail in work [95]). In the first case there were produced spatially aligned multilayer nanotubes several tens of nm in outer diameter closely packed in bundles, which in turn formed thread-like structures up to 3 mm in length and 0.1 mm in diameter. In the second case, the subject of study was a bundle of disordered multilayer nanotubes several tens of nm in outer diameter applied upon a glass substrate. Intercalation was performed in a two-section glass tube. Nanotubes were suited in one section, whereas an intercalated agent was put into another one. Either purified K or anhydrous iron chloride ($FeCl_3$) was used as an intercalated agent. The tube was pumped out and sealed off. The gaseous phase reaction was performed at a temperature of 300 °C in the case of K, and 280 °C in the case of $FeCl_3$. All procedures were carried out in a sealed off chamber in an Ar atmosphere.

As a main result of the publications cited there is the fact to be considered that the intercalation can be performed only in relation to samples produced using the electric arc method. The intercalation reaction did not change either dark colour or thread-like structure of samples, while in the case of $FeCl_3$ some deterioration and disorientation of fibers was observed. The samples were notably put on in weight (15 – 33% in the case of K, and 110 – 260% in the case of $FeCl_3$) and size. The intercalation reaction considerably changes the appearance of nanotubes in a scanning electron microscope. Straight nanotubes become convex as a result of the reaction, especially in the case of $FeCl_3$. The results of X-ray diffraction investigations show that the intercalation causes an increase in the interlayer spacing from 0.344 to 0.53 nm in the case of K, and to 0.95 nm in the case of $FeCl_3$. This proves that the intercalation affects each tube, but not the intertube region. The intercalated nanotubes are shaped into beadline patterns, where the swollen sections alternate nonintercalated 'necks'. These peculiarities can be considered as an evidence that nanotubes produced using electric arc method have the scroll structure and are intercalated not from the end side but from the lateral edge.

The nanotubes produced through the chemical vapor deposition method are not affected by the intercalation reaction in the conditions described above. Therefore, the authors of the experiment conclude that in this case the structure of nanotubes is close to 'Russian dolls' one.

It is well to bear in mind that the perfect transverse structure of nanotubes, where the interlayer spacing is close to 0.34 nm and axially independent, is distorted in practice due to a perturbing action of adjacent nanotubes. This was illustrated in one of the first publications in the field [96], where the electron microscope observations showed 2 – 3% decrease in interlayer spacing in the area of contact between 10-layer and 12-layer adjacent nanotubes. The estimations taking into account van der Waals interaction between atoms confirm this effect quantitatively.

Other deviations from the ideal nanotube structure were observed in works [97 – 101] using the electron microscope and X-ray diffraction methods. Thus, high-resolution electron microscope observations [98, 99] have shown that a considerable portion of multilayer nanotubes has polygonized cross section. In such a structure the plane sections are adjacent to surfaces of high curvature, which contain the edges with a high degree of sp^3-hybridization of carbon. These edges confine the surfaces consisted of the sp^2-hybridized carbon and determine many properties of nanotubes. The impact of sp^3-defects on the ideal structure of the nanotube surface was studied in more detail in works [100, 101]. It was shown, in particular, that the defects cause a distortion in the rectilinear shape of a nanotube, shaping it in a pleat-like structure whose wavelength is 2 – 8 times as large as the six-member ring size.

A great deal of information about the transverse structure of multilayer nanotubes was provided by work [102], where in contrast to the conventional approach the electron beam in diffraction measurements was aligned in parallel to the nanotube axis. Let us consider this work in more detail. Nanotube bundles extracted from a cathode soot were inserted into an epoxide resin with tweezers. After solidification at 60 °C for 3 days the plane samples 20 – 30 nm in thickness were cut from the resin bulk with a diamond knife and observed using a high-resolution electron microscope. The observations show that one end of a tube is usually connected with a piece of the pyrolytic graphite or the polyhedral particle. Another end of a nanotube is closed, while its shape is closer to a cone rather than to a sphere. A wide variety of tube configurations was observed. Thus, the seven-layer tube 2.04 nm (6×0.34 nm) in inner diameter was seen. The interlayer spacing was always close to 0.34 nm. There might be seen also a 32-layer tube having the inner diameter of 3.4 nm (10×0.34 nm). A rise in the number of layers results in an increased deviation from the ideal cylindrical shape of a nanotube. In some cases a polyhedral structure of the outer envelope of a nanotube was observed. Sometimes a nanotube surface was covered with a thin layer of a disordered (amorphous) substance. The ideal closed concentric structure of the cross section was observed in none of the cases.

Both the longitudinal and transverse structures of multilayer nanotubes significantly depend on the production method. As was found in works [76 – 81] using electron diffraction methods, the most wide variety of longitudinal structures is inherent to multilayer nanotubes grown on the surface of metal nanoparticles in response to the catalytic acetylene decomposition. Catalytically grown nanotubes

have usually the inner and outer diameter of several nm and several tens nm, correspondingly, and reach up to several tens of micron in length. About 10% of nanotubes are formed into regular spirals with the radius and pitch varied over wide limits. Tubes curve in an odd manner; they are twisted with themselves and with each other, forming twisted spirals, ropes, loops and all sorts of other structures.

The observations have shown that the interlayer spacing in multilayer carbon nanotubes produced in an arc discharge can change from the standard value of 0.34 nm up to the twice magnitude of 0.68 nm. This points to the existence of defects in nanotubes, where one of the layers is partly absent.

Another sort of defects observed quite often on the graphite surface of multilayer nanotubes is a result of introduction of a number of pentagons or heptagons into such a surface consisted mainly of regular hexagons. The presence of these defects in the structure of nanotubes causes distortions in their cylindrical shape so that the introduction of a pentagon brings about the convex bend, whereas a heptagon produces a concave bend of the ideal cylindrical surface of a nanotube. Therefore such defects result in appearance of curved and spiral-like nanotubes. In this case the existence of spirals with a constant pitch bears witness to more or less regular arrangement of defects on a nanotube surface. This problem was studied in detail, for one, in work [104], where on the basis of observations of bent nanotubes the conclusion was made about existence of seven-member carbon rings in their structure. The nanotubes were produced in conditions typical of fullerene production. A cathode deposit consisted of a black core surrounded with a gray cylindrical envelope. The core was inserted into methanol and ultrasonicated for 10 minutes, resulting in a black suspension. On drying the latter a black powder was obtained, containing nanotubes, polyhedrals and amorphous carbon. The gray envelope of a deposit did not essentially contain nanotubes. Bent nanotubes were observed directly using a high-resolution electron microscope 300 kV in voltage and 0.20 nm in resolution, designed on the base of a field emission microscope. The minimum diameter of the electron beam accounted for 3 nm. There were observed bent nanotubes which showed the occurrence of sections of negative curvature caused by the presence of heptagons or pentagon–heptagon pairs in the graphite structure. The curvature of the nanotube is accompanied by either bending or breaking of a graphite surface.

4. Electrical and magnetic properties of carbon nanotubes

4.1 Electron properties and the nanotube chirality

As noted in the preceding section of the article, the electrical properties of single-layer nanotubes are appreciably determined by their chirality. This follows from a great number of calculations on the density of occupied electronic states for carbon nanotubes [17–24] (see also work [106], which is rather rich in the methodical content). These states are formed as a result of delocalization of $2s$ and $2p$ electrons of a carbon atom, so that $2s$ electrons in hybridization fill energy regions lying below and above the Fermi level, whereas $2p$ electrons fill a region near the Fermi level. As this takes place, a change in chirality and hence in the nanotube radius also causes a change in the energy gap, which is a monotonously decreasing function of the radius as follows from the computational investigation.

For characterization of the nanotube chirality it is convenient to use the index $k = m - 2n$ $(m > 2n)$ instead of the above-introduced indices (m, n), which uniquely determines electron properties of a nanotube with a prescribed radius [21]. For example, a tube with $k = 0$ corresponding to the chirality angle $\theta = \pi/6$, possesses a metallic conductivity; at $k = 3(q+1)$ it is a narrow gap semiconductor, whereas at $k = 3q + 1$ and $k = 3q + 2$ $(q = 0, 1, 2, \ldots)$ it is a semiconductor with a moderate energy gap.

The quantitative relationships defining the interconnections between the chirality indices of an ideal single-layer nanotube, its radius and energy gap can be stated only on the basis of model calculations using rough simplifications. For this reason the results of calculations performed by various authors [17–24, 106] differ from one another in some details, and yet they are characterized by common qualitative features. These features are displayed in Fig. 9, where are shown the dependences of the energy gap ε_g on the reduced tube radius $R_d = R/d_0$ calculated in work [106] for a long single-layer nanotube at various magnitudes of the chirality index k. Here R is the radius of a nanotube, $d_0 \approx 0.14$ nm is the spacing between neighbouring carbon atoms on a graphite plane, and the energy gap ε_g is expressed in terms of the interaction energy $\varepsilon_{pp\pi}$ for two p-electrons belonged to neighbouring carbon atoms in a graphite lattice, the interaction being responsible for the formation of the π bond. This interaction energy is known with a limited accuracy, which imparts a qualitative character to the calculated data presented. The solid line in the figure shows the dependence $\varepsilon_g = 1/R_d$ found by the authors [19] on the basis of a simplified approach without considering the dependence of the interaction energy for p-electrons on the nanotube radius. All model calculations performed up to now show the inversely proportional dependence of the energy gap on the nanotube radius, as well as the metallic nature of electron conductivity of nanotubes with $k = 0$.

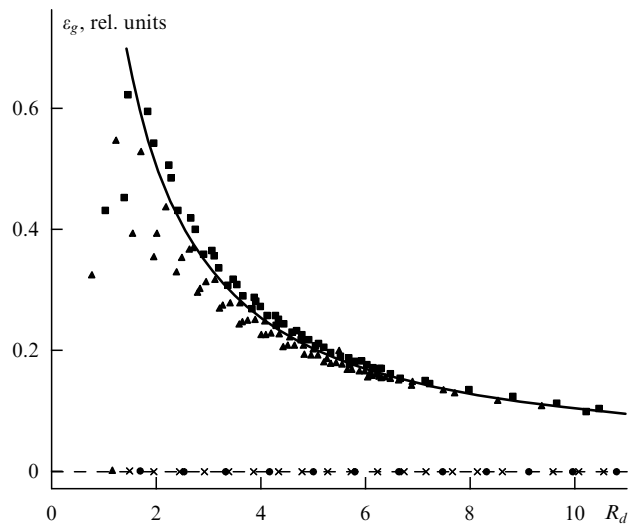

Figure 9. Dependence of the energy gap for a long single-layer nanotube on the reduced radius R_d as calculated in Ref. [106] for nanotubes with various indices of chirality: × — $k = 0$; ● — $k = 3(q+1)$; ▲ — $k = 3q + 1$; ■ — $k = 3q + 2$.

4.2 The conductance of nanotubes

The electrical conductivity of carbon nanotubes is their key parameter, because the prospects of the nanotube usage in a further miniaturization of the microelectronic devices depend on both the value and possibility of measuring this parameter. In spite of numerous efforts mounted in this direction, there are still absent reliable experimental data supporting the above-cited theoretical predictions [17 – 24, 106] about the connection between the conductivity of an individual nanotube and its chirality. This is caused on the one hand with difficulties in producing and identifying nanotubes with a specified chirality, and on the other hand with obstacles to measuring the conductivity of an individual nanotube.

In view of the above-indicated difficulties, in first experiments directed to determining the conductivity of nanotubes there were studied not so much individual nanotubes as materials consisted of a great number of nanotubes having different characteristics. Thus, one of the most substantial works of such a kind [27] deals with the detailed investigation of the electrical and optical characteristics of a film consisting of longitudinally aligned nanotubes. For production of this film [109], the starting soot generated employing the method [6] described above, was ultrasonically dispersed in ethanol, then the suspension was centrifuged and filtrated with a ceramic filter for removing sizable agglomerates. The obtained deposit containing a great quantity of nanotubes was suited onto a teflon substrate. A considerable portion of nanotubes was thus found to be aligned transversely to the teflon layer plane (β-orientation). Gently rubbing the obtained layer of aligned nanotubes with a teflon tape resulted in changing their orientation from transverse to longitudinal in the direction which is parallel to the substrate plane (α-orientation). The electron microscope observations therewith showed that polyhedral carbon nanoparticles remained on the substrate surface along with nanotubes.

The four-probe measurements of temperature dependences of resistivity in nanotube films were performed in the temperature range $0.03\ \mathrm{K} < T < 300\ \mathrm{K}$. As follows from these measurements, the magnitude of resistivity measured in the direction aligned with that of the nanotube orientation R_{par} ranges from 1 down to 0.08 Ω cm. In this case the temperature dependence of the resistivity is close to $T^{-1/2}$. The temperature dependence of the resistivity R_{perp} measured in the transverse direction, is described with the similar function. The resistivity anisotropy $R_{\mathrm{perp}}/R_{\mathrm{par}}$ is close to 8 and practically remains temperature-independent. At temperatures below 0.1 K both the dependences saturate. Comparing the measured results with the below-given data relating to individual nanotubes shows that the resistivity of a nanotube film exceeds considerably that for an individual nanotube, whose resistivity in turn is close to the corresponding magnitude for a graphite. It follows that the resistivity of a nanotube film is determined not so much by nanotubes themselves as by points of the contact between adjacent nanotubes. Thus, the charge transfer is governed by the hopping mechanism. The existence of an anisotropy points to the fact that the number of contact points per unit length in the longitudinal direction is much less than that in the transverse one. A dropping temperature dependence of the resistivity is indicative of the activation character of a hopping charge-transfer mechanism. At very low temperatures the quantum subbarrier tunnelling remains as the main mechanism of conductivity, which limits the resistivity magnitude. Processing experimental data provided the estimations for the height of a potential barrier (10 meV) and the length of a jump (10 nm).

In the same work [27] the temperature dependences of the Hall coefficient for longitudinal and transverse alignment of nanotubes in a film were also measured. The data obtained in the same temperature range show a smooth fall in this parameter approximately from 0.4 to 0.1 $\mathrm{cm^3\ C^{-1}}$ at a slight anisotropy. Processing of these data provides an upper estimate for the carrier concentration ($1.6 \times 10^{19}\ \mathrm{cm^{-3}}$), which permits us to believe that the nanotube film, like the graphite, can be related to semimetals.

A more sharp drop in the temperature dependence of nanotube resistivity was observed in works [110 – 112], where individual multilayer nanotubes normally bound in bundles were studied. The material produced using a standard method [6] contained a number of nanotube bundles and a multitude of single tubes about 18 nm in diameter. This material was suited on a silicon oxide substrate, a notable part of which was covered with a set of gold pads. After evaporation of a thin gold film, a few layers of a negative electron resist were deposited onto the substrate employing the Langmuir – Blodgett procedure. Then with a scanning electron microscope there was removed the resist layer situated between the nanotube and predefined gold pads. The rest of the Langmuir – Blodgett film was removed through the dissolution in ethanol and unprotected parts of the gold film were removed via the Ar-ion etching. By this expedient 4 electrically connected nanotubes or bundles were obtained. The measurements of electrical properties were performed with a tube 20 nm in diameter at the distance between the contacts equal to 800 nm. The temperature dependences of conductivity are presented in Fig. 10. The conductivity is proportional to the logarithm of the temperature at $T \geqslant 1$ K and saturates at lower temperatures.

The conductivity of nanotube bundles is changed significantly as a result of doping with electron acceptors or

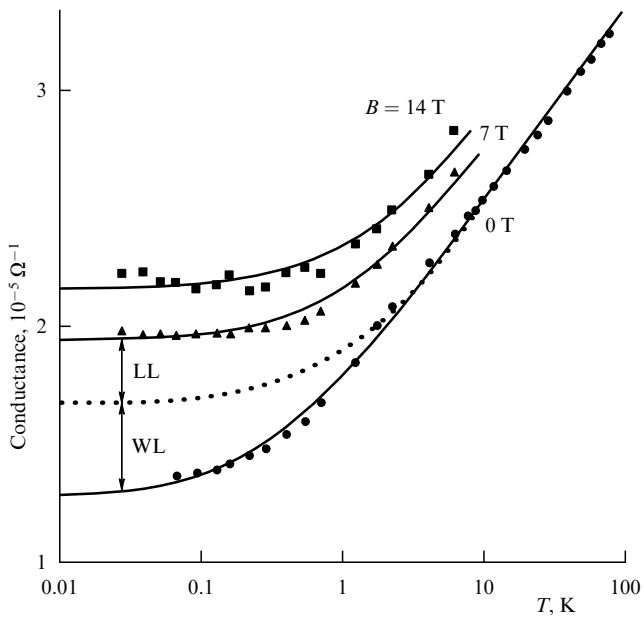

Figure 10. Temperature dependences of the conductance for an individual multilayer carbon nanotube 200 nm in length and 20 nm in diameter as measured in work [110] at different intensities of the magnetic field. The arrows show the contribution of a weak localization (WL) and Landau levels (LL) to the magnetoresistance.

donors. This effect which is similar to that for fullerenes, was clearly demonstrated in work [92], where doped bundles of single-layer nanotubes with a predominant chirality (10,10) were studied. The procedure of producing the pristine bundles using two laser beam irradiation of a graphite surface in the presence of bimetallic catalyst was described in detail above (see Section 2.4) [71]. Br_2 played a part of the electron acceptor, whereas atomic K did that of the electron donor. As stated in the experiments, doping the nanotube bundles with Br_2 in rough stoichiometry $C_{52}Br_2$ results in dropping the room-temperature resistivity of a nanotube bundle sample from 0.016 down to 0.001 Ω cm. The resistivity weakly depends on the temperature and increases by about 50% as the temperature rises from 150 up to 450 K.

Potassium doping in rough stoichiometry KC_8 provides the room-temperature overall reduction in resistivity by a factor of ~ 20. A weakly rising temperature dependence of resistivity in the temperature range 100–300 K is also observed. This latter feature shows the metallic character of conductivity relevant to doped nanotube bundles. As follows from the Raman scattering measurements [136], the change in conductivity of nanotube bundles under doping is caused by charge transfer between the electron donors (acceptors) and the nanotubes. This is an indication of the ionic character of conductivity, so that intercalation enhances the carrier concentration in samples.

The detailed investigation of the conductivity of individual nanotubes was performed by the authors of the excellent work [115] using an original four-probe method of measuring. Nanotubes were produced by the standard electric arc method and to improve the quality they were annealed in the Ar atmosphere at $T = 3120$ K for 15 minutes. Then they were deposited onto a silicon oxide surface in the region between gold pads. Nanotubes 2–4 μm in length were visualized after irradiating the surface with the Ga ion beam 30 keV in energy and 4 pA in current, which provided the surface fluence at a level of 2×10^{14} cm^{-2}. The conductivity was measured employing the four-probe method, in accordance to which 4 tungsten conductors 80 nm in thickness were deposited onto the nanotube-containing substrate surface as shown schematically in Fig. 11. The deposition was performed with an ion-induced method using gaseous $W(CO)_6$ for the W carrier. The conductors each were connected to one of the gold pads. The distance between contacts on the nanotube ranged from 0.3 to 1.0 μm. The results of measurements are compiled in Table 4. As is seen, the resistivity of nanotubes is varied over a wide range. The minimum value of the nanotube resistivity (5.1×10^{-6} Ω cm) is about an order of magnitude as low as that ($\approx 3.8 \times 10^{-5}$ Ω cm) [116] for crystal graphite, measured in the transverse direction (along a graphite layer plane). The measured temperature dependences of nanotube resistivity are also remarkable for their diversity. Some of them are shown in Fig. 12. Both rising and dropping dependences are evident. The sharpest decrease in the resistivity with temperature is observed for nanotube No. 6, which has the least value of the resistivity. Nanotubes Nos. 2, 3, 7 and 8 are characterized by the most smooth (decreasing) temperature dependences. The analysis of the latter shows that the nanotube energy gap does not exceed 0.1 meV. It permits us to believe that in spite of the considerable spread in the absolute magnitudes of resistivity, the conductivity of nanotubes under consideration exhibits a common metallic nature. The conductivity of nanotubes Nos. 1, 4 and 5 is hardly of a metallic nature. It follows firstly from the higher absolute magnitudes of resistivity and, secondly, from a more sharp decrease in the temperature dependence of the nanotube resistance (presented in Fig. 12b on a semilogarithmic scale), which is an indication of the activation nature of this dependence. The estimations of energy gap for nanotubes Nos. 4 and 5, performed on the basis of these measurements, result in the values of 0.1 and 0.3 eV, correspondingly.

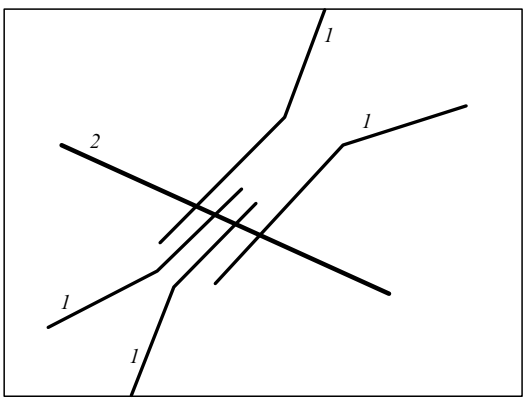

Figure 11. Schematic of the resistance measurements taken for individual nanotubes using the four-probe method [115]: *1* — tungsten contacts 80 nm in thickness; *2* — the nanotube.

Table 4. The four-probe room-temperature measurements of the conductance of various nanotubes [115].

No. of the tube	Radius, nm	The distance between contacts, μm	Resistance, Ω	Resistivity, Ω, μm^{-1}	Resistivity, Ω cm
1	5.0	1.0	$\geqslant 10^8$	$\geqslant 10^8$	$\geqslant 0.8$
2	10.2	0.3	10.8×10^3	3.6×10^4	1.2×10^{-4}
3	~ 3.0	0.35	10.5×10^3	3.0×10^4	7.5×10^{-5}
4	6.3	0.5	2.4×10^8	4.8×10^8	5.8
5	3.6	0.9	$\geqslant 10^6$	$\geqslant 10^6$	$> 4 \times 10^{-3}$
6	9.10	1.0	2.0×10^2	2.0×10^2	5.1×10^{-6}
7	6.1	0.5	4.3×10^4	8.6×10^4	9.8×10^{-4}
8	7.4	0.5	6.0×10^5	1.2×10^4	2.0×10^{-4}

Some difference between the results of the work considered [115] and works [110–112] cited above is noteworthy, with the conductivity of individual nanotubes being measured in the latter works using the two-probe method. In contrast to work [115], where a slight positive magnetoresistance and smoothly rising temperature dependence of the nanotube resistivity were observed, in the cited works [110–112] a notable negative magnetoresistance and a logarithmic decrease in the resistivity with temperature ($R(T) \approx -\log T$) were found. This fact is in conflict with the above-indicated measurement data showing the pronounced negative magnetoresistance of nanotubes. Such a contradiction is an indication of a great diversity of nanotube types with different properties, the latter being appreciably dependent on the conditions of their production.

One more contradiction inheres in the experimental data concerning the conductive properties of nanotubes and it is related to the difference in the conductivity of individual nanotubes and bundles consisted of a great number of nanotubes. As follows from work [120], where transport and magnetic characteristics of nanotube films were measured, the inherent resistance of nanotubes (estimated using the

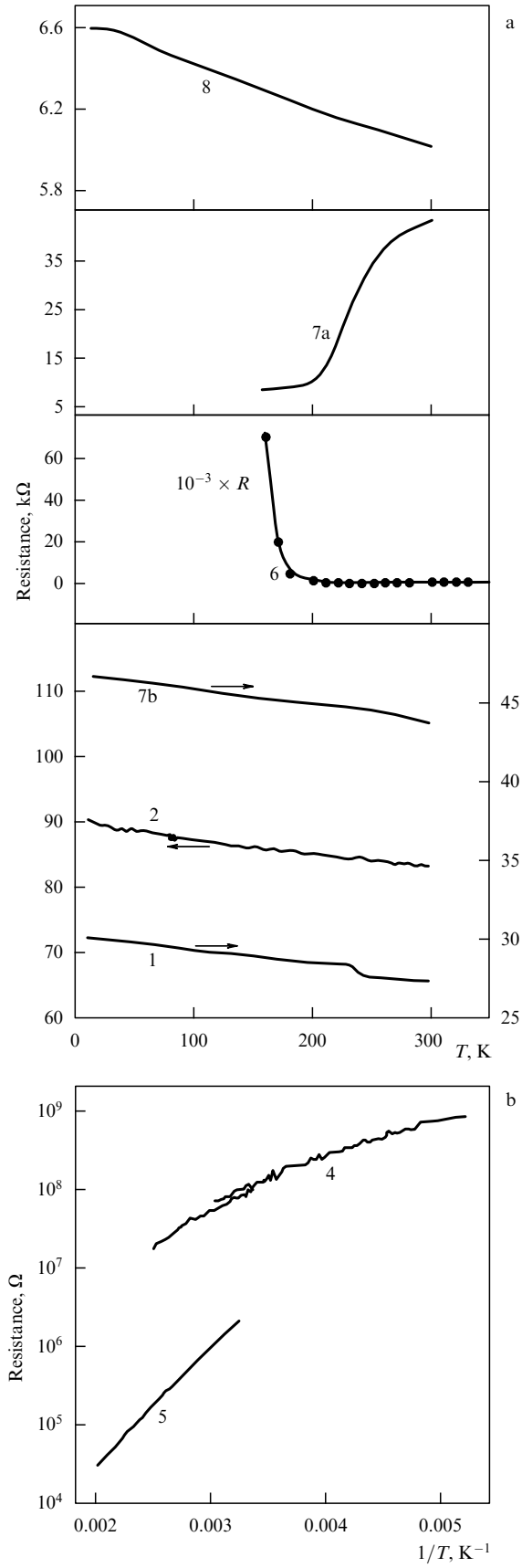

Figure 12. Temperature dependences of the resistance of individual nanotubes as measured using four-probe (a) and two-probe (b) methods in work [115]. The nanotube serial numbers placed alongside the curves in the figure are consistent with the data in Table 4.

measured linewidth of electron spin resonance) is two orders of magnitude lower than that based on direct four-probe measurements. This confirms a decisive importance of intertube contacts for the film resistance, which has been also noted by the authors of work [121].

The noted ambiguity in electrical and magnetic characteristics of individual nanotubes is, in a considerably less degree, inherent to single-layer nanotubes with the predominant chirality (10,10). Such nanotubes are produced through the laser vaporization of graphite in the presence of Ni/Co catalyst, as was described in detail above [71]. This procedure makes it possible to produce nanotube samples 1.38 nm in diameter and of the order of micrometer in length with a predominant armchair structure. The room-temperature conductance of individual nanotubes of such a kind was measured in work [117], where a nanotube sample 3 μm in length was used. The measurements performed at the distance 140 nm between the contacts, resulted in the resistance of 550 kΩ. The contact resistances are estimated as 300 kΩ at room temperature and 1 MΩ at 4 K. The analysis of current-voltage characteristics obtained at different magnitudes of the bias voltage bears evidence of the quantum nature of the nanotube conductivity. The conduction proceeds between clearly distinguishable electronic states, for which the length of the coherent interaction exceeds at least the distance between contacts (140 nm).

4.3 Emission characteristics of nanotubes

The possibility for the nanotube to be used as a source of a field electron emission is of considerable scientific and applied interest. This property centres around the extraordinary low cross section of nanotubes, which provides a sizeable enhancement of the electric field strength near the nanotube cap in relation to that averaged over the entire volume of the interelectrode gap. The measured emission characteristics of nanotubes aligned normally to the substrate plane are presented in Fig. 13, where is shown the dependence of the emission current on the applied voltage [27, 108]. At a voltage

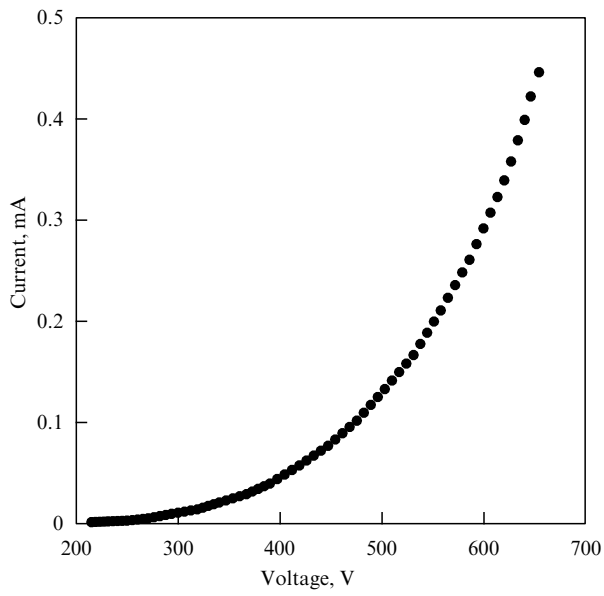

Figure 13. The current-voltage characteristic of the field emission from the film containing nanotubes aligned normally to the substrate plane [27]. The emitted area is about 1 mm^2.

near 500 V, the emitting area of about 1 mm^2 provides the emission current of order 0.5 mA. These data correlate well with the known Fouler – Nordheim expression

$$I = CE^* \exp\left(-\frac{K\varphi^{3/2}}{E^*}\right).$$

Here C and K are the constants, φ is the work function of an emitting surface, and E^* is the electric field strength at the point of the electron emission. Since this point is situated close to the sharpened top of the nanotube cap, the indicated local magnitude of the electric field strength E^* considerably exceeds the mean value of E. Thus, the known effect of the field enhancement is involved, the magnitude of which E^*/E is estimated to be of order 1000, assuming the work function to be close to $\varphi = 5$ eV (characteristic of a graphite surface). This circumstance recommends the nanotube films for application in electronics as the active component of an electron gun.

The measurements of the emitted electron energy distribution function showed that at low emission currents it consisted of separate peaks about 0.12 eV in width, which were assigned to the emission from individual nanotubes. A rise in the emission current resulted in overlapping these peaks, so that the spacing between them stayed at a level of 0.1 – 0.2 eV. This fact shows the differences in the location of discrete electronic levels of various individual nanotubes in relation to the Fermi level.

The emission properties of nanotubes were also studied in works [29, 118, 119], where nanotubes manifested themselves not only as a source of the electron field emission, but also as a source of an intense thermoelectron emission at relatively low temperatures. Nanotube films were produced by employing two methods [29, 119]: one of them is based on the vaporization of a graphite in a vacuum under the action of an electron beam followed by the deposition of carbon atoms onto a substrate, and the second one involves the plasma deposition in deciding on proper conditions. There were separately studied single-layer nanotubes 0.8 – 1.1 nm in diameter bent into bundles 10 – 30 nm in diameter, which were suited onto a quartz substrate, and multilayer nanotubes 10 – 30 nm in diameter suited onto a silicon substrate. The thickness of films ranged between 0.2 and 0.4 μm. In the experiments aimed at studying the emission properties of nanotubes, a molybdenum rod 0.6 mm in diameter (spaced 15 μm apart from the film surface) was used as an anode. The electron field emission of single-layer nanotubes was observed at the electric field strength exceeding 16 V μm^{-1}; the emission current density therewith accounted for 0.03 A cm^{-2}. The current-voltage characteristic of the emission process is adequately described by the well-known Fowler – Nordheim equation, thus attesting to the field origin of the emission. The maximum attainable magnitude of the field emission current density reaches 3 A cm^{-2}, which is comparable with the best results obtained for the diamond-like films. The field emission of multilayer nanotubes is possible at higher magnitudes of the electric field strength, however about the same magnitudes of the emission current density as in the case of single-layer nanotubes are attainable in the process. Processing current-voltage characteristics of the electron field emission permitted the authors to estimate the electron work function for the film surface. This value appeared to be 1 eV, which enables us to consider nanotubes as one of the best materials for use in electron guns. In the experiments related to the study of thermoelectron emission, the nanotube film surface was heated with an infrared lamp. A contribution of the thermoelectron emission becomes remarkable at a film surface temperature of 473 K, and predominant at 723 K.

4.4 Magnetic properties of nanotubes

One of the remarkable peculiarities of nanotubes is a clearly pronounced dependence of their electric conductivity on the magnetic field. In the majority of experiments, a rise in the conductivity with the magnetic field is observed. This can be seen, for instance, from the temperature dependences of the conductance of an individual nanotube measured at various magnitudes of the magnetic field and presented in Fig. 10. In Fig. 14 are shown (in relative units) the dependences of the magnetic addition to the conductance on the magnetic field, measured at various temperatures (in K). An observed rise in the nanotube conductance with the magnetic field is in agreement with the model concept [113], in accordance with which the magnetic field aligned normally to the axis of a sample provides the formation of a Landau level at the point of crossing of the valence band and conduction band. This results in a rise in the density of states on the Fermi level, promoting an increase in the conductivity. It is expected in the framework of the given model that the magnetoresistance is not temperature dependent at low temperatures and decreases with temperature at temperatures greater than or of order the Landau level width. Such a behaviour is consistent with the results of measuring the resistivity of multilayer nanotube bundles of about 50 nm in diameter performed by the authors of work [112] and presented in Fig. 15. It is found that the resistivity of a bundle considerably depends on the processing temperature for nanotubes. So, a change in the processing temperature from 1000 to 3000 K promotes a decrease in the resistivity of nanotubes produced through the deposition, from 10^{-5} to 10^{-6} Ω m. The features observed in the temperature dependences of conductance and magnetoconductance of nanotube bundles at $T < 2$ K appear to be unexpected and call for clarification. In this temperature

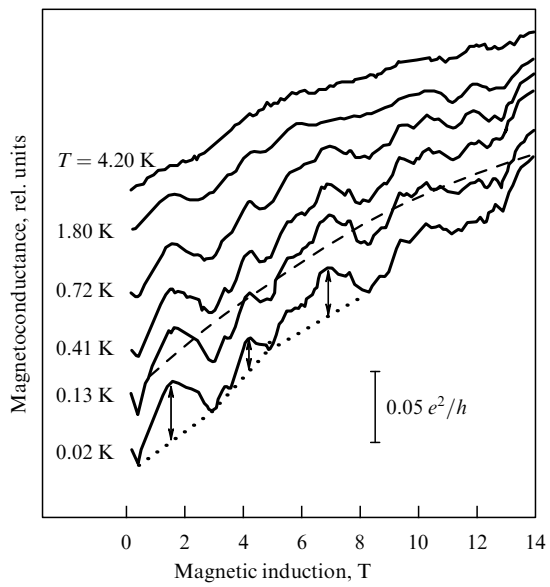

Figure 14. Dependences of the magnetic addition to the conductance of an individual multilayer nanotube 200 nm in length and 20 nm in diameter on the magnetic field, measured at various temperatures in work [110].

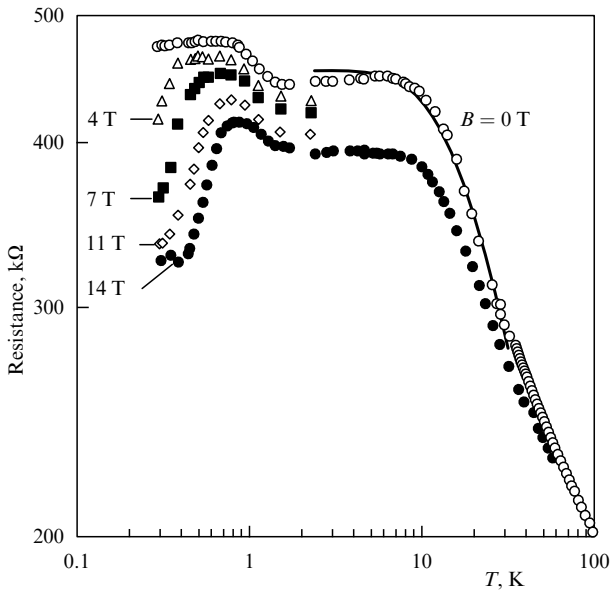

Figure 15. Temperature dependences of the resistance of a single nanotube bundle 50 nm in diameter, measured in work [112] at various intensities of the external magnetic field.

range, a trend towards the stable rise in the conductance with temperature is overlapped with fluctuations assigned to the processes of the interference of electrons in a specific sample exposed to the transverse magnetic field (Aharonov – Bohm effect). The similar data relating to the dependences of the nanotube bundle conductance on the temperature and external magnetic field were also obtained in work [114], where the resistivity of nanotube bundles several tens of nanometers in diameter accounted for 0.65×10^{-4} and 1.6×10^{-4} Ω m at $T = 300$ K and 5 K, correspondingly.

Of strong interest is the character of changes in the electrical and magnetic properties of nanotubes as a result of their doping with metal atoms. The interest to this problem is stimulated by the discovery of a high-temperature (up to 40 K) superconductivity of crystal fullerenes doped with alkali metal atoms and the relevant hopes for revealing the similar phenomena in the case of nanotubes. Detailed measurements of the magnetoresistance of multilayer nanotubes closely packed into bundles several tens of nm in outer diameter and doped with the potassium, were performed in works [122, 93]. The samples studied represented nanotube bundles, forming thread-like structures up to 3 mm in length and 0.1 mm in diameter. The procedure for preparing samples under consideration was described in detail above (see Section 3.4).

The intercalated material is rather sensitive to the air humidity. Due to the hydrolysis, the intercalation process is completely reversed on allowing to stand in air for several days. After washing with water and drying such reintercalated tubes are completely restored to their initial appearance, when observed with a microscope.

The samples show the negative magnetoresistance at $T = 1.8$ K. In contrast to the initial sample, for which oscillations in the magnetoresistance versus the magnetic field are observed, for intercalated samples this dependence is smoothly decreasing. The material is produced in a graphite-electrode arc discharge burning in He atmosphere. Bundles formed fiber structures 1 – 3 mm in length and about 0.1 mm in diameter, which were terminated at electrical contacts. The conductance was measured before and after intercalation by the standard two-probe method with the magnetic field oriented normally to the axis of a sample. The measured temperature dependences of the conductance of initial and intercalated samples are compared in Fig. 16. As seen, this dependence for the initial sample at $T < 10$ K has a form typical of semiconductors ($G \propto \ln T$). Doping nanotubes with K atoms promotes considerable changes in the temperature and magnetic field dependences of the nanotube conductance (see Figs 16, 17). In contrast to the graphite, the conductance of which in the direction of a graphite plane increases by 4 orders of magnitude due to doping with K

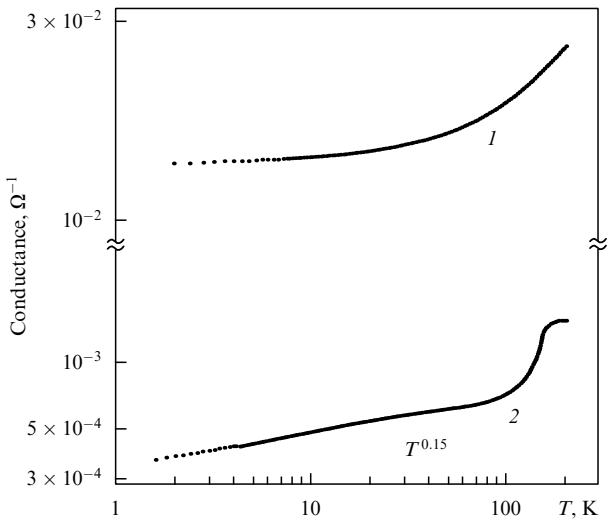

Figure 16. Temperature dependences of the conductance of a nanotube bundle 1 – 3 mm in length and about 0.1 mm in diameter, measured before (*1*) and after (*2*) intercalation with K atoms [122, 93]. The weight content of K in the sample ranges into 15 – 30%.

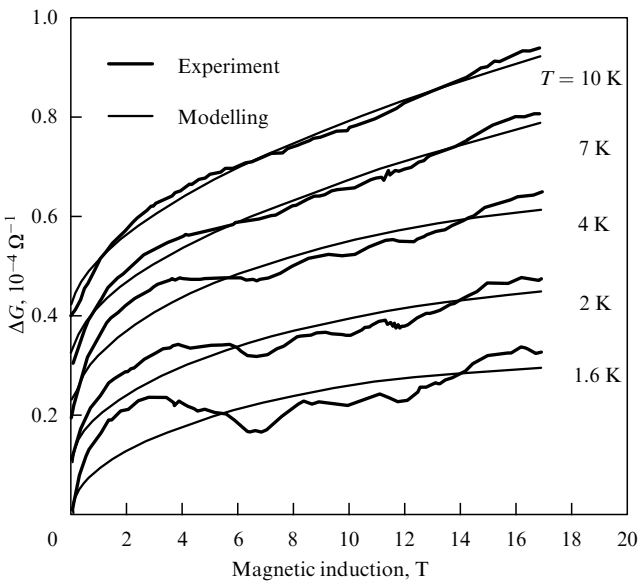

Figure 17. Dependences of the magnetic addition to the conductance of the K-doped nanotube bundle 1 – 3 mm in length and about 0.1 mm in diameter on the intensity of the magnetic field, measured at various temperatures [122, 93]. The weight content of K in the sample ranges into 15 – 30%. For the sake of convenience, each curve has been sequentially shifted in a vertical direction by 10^{-5} Ω^{-1}.

[124], the conductance of nanotube bundles decreases by 2 orders of magnitude as a result of K doping, remaining to be increasing with temperature. It appears to be explicable not so much through a decrease in conductance of individual nanotubes as by disordering in their mutual arrangement and weakening in their interconnection. At $T < 100$ K, $G \propto T^{0.15}$; it rises sharply at $T = 100$ K and becomes time-dependent at higher temperatures.

Figure 17 displays the addition to the conductance of a nanotube bundle (doped with potassium) caused by the action of the magnetic field, versus the magnitude of this field, measured at various temperatures [122, 93]. These dependences represent a smoothly rising function overlapped with oscillations, which are similar to those observed in studying an individual multilayer nanotube [110] (see Fig. 14). The presence of oscillations points to the coherent character of the charge transport over a considerable part of the sample volume.

An important parameter characterizing the magnetic properties of a material, is its magnetic susceptibility. The measurements of this parameter for nanotube bundles were performed in works [123, 125, 126]. Figure 18 compares the measured results [125] with corresponding data for other carbon forms. The measurements were performed with a SQUID magnetometer. The nanotubes bound in bundles of disordered orientation were produced in an arc discharge with graphite electrodes burning in the He atmosphere. The large negative magnetic susceptibility of nanotubes shows their diamagnetic properties. It can be supposed that the diamagnetism of nanotubes is caused by the electron current flowing along their circumference. As follows from the measurements, the magnitude of χ does not depend on the orientation of a sample, which is an indication of its disordered structure. Rather high magnitude of χ is evidence that at least in one of the directions this value is comparable with that for a graphite or exceeds it. The striking difference in the temperature dependences of the magnetic susceptibility for nanotubes and other carbon forms can be considered as one more evidence that the carbon nanotubes exhibit the individual, original carbon modification, the properties of which are basically differed from that of a carbon in other states.

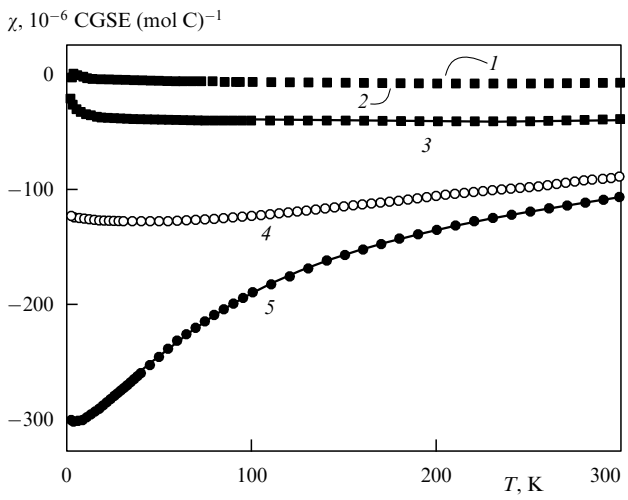

Figure 18. Temperature dependences of the magnetic susceptibility χ of various carbon modifications (averaged over orientations) [125]: *1* — crystal fullerene C_{60}; *2* — diamond; *3* — activated charcoal; *4* — highly oriented pyrolytic graphite; *5* — nanotubes.

5. Nanotube applications

5.1 Technological applications of nanotubes

The above-described physical and chemical properties of carbon nanotubes permit the consideration of this object as a material with unique characteristics, which can be used as the base for diverse applications of this substance. It should be taken into account that at the present time the net world annual production of nanotubes ranges up to several kilograms, thus determining their rather high market prices (at a level of hundred dollars per gram). In such a situation the matter of a possibility of large scale practical applications of nanotubes should be considered as their production is risen and consequently their price is lowered. Notice that the similar situation takes place in the case of fullerenes, which are distinguished however with about an order of magnitude higher world net production. In connection with these remarks we shall consider below some potentialities of nanotube applications, based on results of investigating their chemical and physical properties and also on the data of preliminary experiments. The problem of the practical realization of these possibilities can be solved from the development of corresponding technologies for large scale nanotube production at relatively moderate prices.

Many technological applications of nanotubes are based on their high specific area. The trend of nanotubes towards the formation of multiply twisted with each other and randomly oriented spiral-like structures results in the occurrence (inside the nanotube material) of a large number of nanometer-sized cavities attainable for penetration of gases and liquids from the outside. In response to this trait the specific area of a material consisted of nanotubes becomes to be close to that for an individual nanotube. This value in the case of a single-layer nanotube accounts for about 600 $m^2\,g^{-1}$. Such a high magnitude of the specific area of nanotubes provides a possibility for their use as a porous material in filters, apparatus of chemical technologies, etc.

Recently published work [31] can be considered as one of the indicative examples showing a possibility of the effective application of nanotubes in the chemical technologies, using the nanotube material as a support for performing heterogeneous catalysis. To fabricate the catalyst, the mixture of 1 g nanotubes and 20 ml HNO_3, containing 1.25 g dissolved $Pd(NO_3)_2$ (8% Pd), was conditioned in an oil bath at $T = 120\,^\circ$C for 24 h. After drying in an oven at $T = 100-120\,^\circ$C for 3–12 h the material was reduced in the flowing hydrogen (20 ml min^{-1}) as the temperature increased from the room level up to 250 °C at the rate of 10 °C min^{-1} and then was held at $T = 250\,^\circ$C for 3.5 h. The catalyst produced in such a manner contained 10 wt. % of Pd. The nickel and ruthenium catalysts on a nanotube substrate were prepared in the same fashion. The specific area of opened and closed nanotubes as determined through the physical sorption of N_2 at $T = -196\,^\circ$C was found to equal 21 and 36 $m^2\,g^{-1}$, correspondingly. The catalytic ability of metals suited onto a nanotube substrate were studied for the cases of the reactions of liquid-phase hydrogenation of *p*-nitrotoluene and gas-phase hydrogenation of CO. In the first case 0.23 g of Pd suited on a nanotube substrate were mixed with 1.377 g of *p*-nitrotoluene dissolved in 100 ml of methanol. The reactor

was quickly heated from room temperature up to $T = 100\,^{\circ}\mathrm{C}$ and held at that temperature in the H_2 atmosphere at a pressure of 14.5 bar for one hour. After that the reaction was terminated in a water bath at room temperature. The gas-phase hydrogenation of CO was performed in a quartz tube 4 mm in diameter filled with 0.05 g of a metal suited on a nanotube substrate through which the mixture of Co/H_2 in the ratio 1 : 14.4 at atmospheric pressure and the temperature lying between 300 and 350 °C was pumped. The experimental data show that the hydrogenation of *p*-nitrotoluene (4-nitromethilbenzene) to *p*-toluidine (4-methylaniline) using 10% mixture of Pd with opened nanotubes in methanol results in 75% conversion without formation of by-products. For closed tubes this factor accounts for 61.7%. The data related to the grade of the conversion under gas-phase catalytic hydrogenation of CO to CH_4 and H_2O using 10% mixture of various metals with opened and closed nanotubes at $T = 300\,^{\circ}\mathrm{C}$ are given in Table 5. These data are compared with the catalytic activity of a catalyst on the base of a graphite. As may be seen, the catalytic efficiency of opened nanotubes notably exceeds that for closed nanotubes and a graphite. The high-resolution electron microscope observations show that palladium particles attached to a nanotube surface are of about 5 nm and less in size, with particles of lesser size filling opened nanotubes. The enhanced catalytic activity of opened nanotubes is caused, in the authors' opinion, by the presence of metal particles inside nanotubes, which promotes the catalytic reaction. The high catalytic activity of noble metals held on the nanotube walls has been also demonstrated in relation to the reaction of hydrogenation of diphenylacetylene [127] and cinnanaldehyde [128].

Table 5. The efficiency of various nanotube-based catalysts in relation to the reaction of the catalytic gas-phase hydrogenation of CO [31].

Catalyst	The depth of CO conversion, %
10 % Ru on opened nanotubes	99.9
10 % Ru on closed nanotubes	25.0
10 % Ru on a graphite	5.5
10 % Ni on opened nanotubes	88.6
10 % Ni on closed nanotubes	66.3

An interesting opportunity for using the nanotubes in the technology of the growth of nanocomposite structures was demonstrated in work [129], where nanotubes served as removable templates for production of ceramic structures. Nanotubes synthesized using the standard electric discharge method were dispersed and partially oxidized in air or nitric acid for opening the caps. Then the sample was dispersed and mixed with a pure powder of V_2O_5 in the weight ratio 1 : 1. The mixture obtained by this expedient was heated in an oven up to 750 °C (melting point of the vanadium oxide is equal to 690 °C) and held in air at this temperature for 20 min. The resulting black mixture was crushed and dispersed in ethanol, and then after drying was observed employing the scanning (STEM) and transmission (TEM) electron microscopes. The observations showed that a considerable portion of opened nanotubes is filled with the vanadium oxide.

The filling material is 1 – 2 nm in diameter and up to several hundred nm in length. In tubes with the inner diameter less than 3 nm the filling material has an amorphous structure and high porosity. Tubes of larger diameter are filled with monocrystallic vanadium oxide aligned in a certain manner in relation to the tube axis. Along with filled nanotubes there appeared to be those covered from outside with vanadium oxide thin film no more than 1 nm in thickness. The 'sandwich' structures filled inside and covered from outside with vanadium oxide were observable as well. A film covering nanotubes from outside is uniform throughout the depth. A covered section of a nanotube can reach several hundred nm in length. Very thin nanotubes (less than 5 nm in diameter) as well as nanotube caps remain uncovered. The penetration of vanadium oxide into inner regions of multilayer nanotubes is also observed, where one or several layers are partly absent (it is caused by defects formed either during the growth of nanotubes or on their partial oxidation).

The repetition of the oxidation procedure for nanotubes covered externally with vanadium oxide results in the partial removal of the nanotube interior, i.e. in the enlargement of the hollow inner cavity, remaining several outer layers covered from outside with an oxide film to be invariable. Further oxidation provides the total removal of graphite layers, as a result of which there may be left hollow cylindrical structures of vanadium oxide as well as rods consisted of the same material which filled earlier the inner volume of a nanotube. Thus the nanotubes are used as removable templates in the production of thin-layer ceramic nanostructures.

One more interesting experiment, using the high specific area of a nanotube material, is described in work [130]. In this work carbon nanotubes were employed as electrodes for high-capacity and high-specific-power electrochemical capacitors. The main requirements imposed upon an electrode material for an electrochemical capacitor are related to its high porosity as well as to high resistivity of both the material and liquid electrolyte filling a porous structure of an electrode. As stated from the experimental data involved, carbon nanotubes meet the listed requirements quite well. Nanotubes under investigation were grown using the earlier-developed method of catalytic cracking of hydrocarbons. Multilayer nanotubes produced were about 8 nm in outer diameter and contained a negligible quantity of easily removable admixtures. The high-resolution electron microscope observations show that the majority of nanotubes are bound in bundles of about 2 μm in diameter and of order 20 μm in length. For preparation of electrodes, the nanotubes incorporated into bundles were separated from each other through the ultrasonic dispersing in nitric acid, followed by the attachment to them of the functional chemical groups $-COOH$, $-OH$ and $>C=O$. The subsequent integration of nanotubes resulted in the formation of a continuous interconnected structure. The electrochemical capacitor electrodes fabricated on the base of this structure are 8.3 cm in diameter and about 0.0025 cm in thickness. The electrodes are uniform over the thickness, reproducible, smooth surfaced and offer high mechanical strength. They are flexible and can be easily cut to different shapes and sizes. The density of the electrode material accounts for 0.8 g cm^{-3} and can be varied by changing the production conditions. Other attractive properties of the electrode material, unattainable with conventional materials, are its highly developed porous structure; large specific area easily accessible for an electrolyte; high thermal and chemical stability. As follows from the measured data, the total specific volume of pores in the material accounts for 0.79 $cm^3\ g^{-1}$. The mean diameter of pores is 9.2 nm, whereas the contribution of micropores less than 2 nm in diameter does not exceed 0.2%. The specific area of the electrode material accounts for 450 $m^2\ g^{-1}$. Although this magnitude is

less than that for the activated charcoal (1000 m^2 g^{-1}), the lack of micropores makes the surface to be considerably more accessible for an electrolyte, which promotes the formation of the double layer. The capacitor specimen, designed for detailed testing, consisted of nanotube-based electrodes 1.25 cm in diameter and 0.0025 cm in thickness. The electrodes were separated from each other with a polymer film 0.0025 cm in thickness. As an electrolyte was used 38 wt. % solution of H_2SO_4. The resistivity of the electrode material was measured as 1.6×10^{-2} Ω cm. The dc specific capacitance of the capacitor accounted for 104 F g^{-1}. The equivalent series resistance of the cell came to 0.094 Ω. As follows from measuring the frequency characteristics of the device, essentially total energy stored in a capacitor can be extracted without loss at a frequency less than 100 Hz. In relation to this factor, the capacitor of the type involved is much better than the conventional devices of the same kind, not containing nanotubes. The typical magnitude of the limiting frequency for those devices does not exceed 6 Hz. The energy characteristics of the capacitor developed are also quite impressive. Thus, the specific power of the device exceeds 8 kW kg^{-1} with the specific energy storage at the level of 1.5 kJ kg^{-1}. All these parameters permit us to consider the nanotube-based electrochemical capacitors as highly efficient devices competitive with the best commercial specimens.

Carbon nanotubes, like other carbon modifications, have manifested themselves quite well in the experiments aimed at their usage as a coating which promotes the diamond film formation [131]. In the work cited quartz wafer plates $20 \times 15 \times 1$ mm in size, ultrasonically purified and polished with a diamond paste were used as substrates. The substrates were covered with either the nanotube film or C_{60} or C_{70} or were not covered at all. The diamond films were coated through the gas-phase thermocatalytic reaction of CH_4 and H_2, using a resistively heated tungsten filament as a catalyst. In the experiment, the power supplied to the filament and the time of deposition were varied. The deposition during 4 hours resulted in the formation of a diamond film detected via the Raman spectra. The electron microscope photos showed that the diamond film deposited onto the nanotube film was distinguished for better density and uniformity of embryos if compared with the film deposited onto C_{60} and C_{70} fullerenes. In the latter case, the higher content of an amorphous phase on the boundary of diamond microcrystals was observed.

The prospects of nanotube usage in chemical technologies are appeared to be quite encouraging. This is dictated, on the one hand, by their high specific area and chemical stability and, on the other hand, by the possibility of the attachment of various radicals to the nanotube surface, which can serve later either as catalytic centres or as embryos for performance of diverse chemical transformations. The particular studies directed to the realization of these possibilities are still at an initial stage, however there is no question that new interesting opportunities of nanotube applications in chemical technologies would appear in the nearest future. In one of the first experiments performed in this direction [132] there is shown that as a result of the nanotube oxidation its surface is covered with adducts (–COOH), (–CO) and (–COH) in the ratio 4:2:1. These functional groups can be used as the base for chemical reactions of attachment for a great number of elements and functional groups. As an example, in the article are presented the microphotos of a nanotube decorated from outside with a lead oxide. Thus, there appeared to be opened a possibility for production of a new class of heterogeneous materials around the nanotubes, the surface of which represents a metal oxide bonded to a substrate by rather weak chemical interaction.

5.2 Nanotube applications in electronics

Though technological applications of nanotubes, based on their high specific area, are of a considerable applied interest, as the most attractive there are directions of nanotube usage to be considered, relating to developments in various fields of modern electronics. Such properties of nanotubes as their small sizes variable in a wide range depending on the synthesis conditions, mechanical strength and chemical stability permit one to consider those as the base for elements of microelectronics of the next generation. A possible outline of one of such elements is analyzed in detail in work [133]. The authors have shown through calculations that the incorporation of a pentagon – heptagon pair as a defect into a single-layer nanotube of ideal structure (Fig. 19) changes its chirality and as a consequence its electronic properties. There was considered specifically the structure (8, 0)/(7, 1). As follows

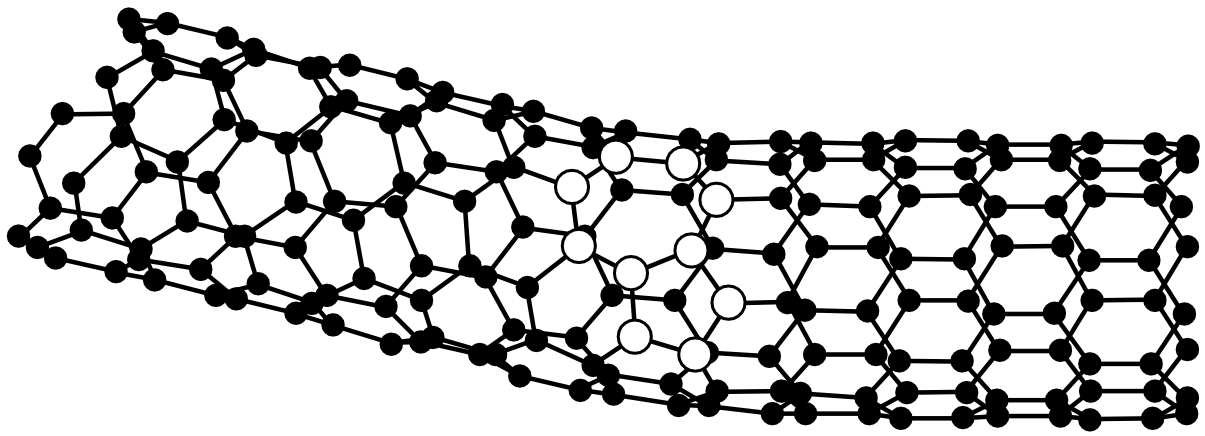

Figure 19. The structure of a heterojunction on the base of a single-layer nanotube with the changed chirality [133]. The empty circles denote carbon atoms forming the pentagon – heptagon defect in an ideal nanotube structure. The occurrence of the defect gives rise to a change in the chirality from (8, 0) to (7, 1).

from the calculations, the tube with chirality (8, 0) exhibits a semiconductor with the energy gap of 1.2 eV, whereas that of (7, 1) chirality is a semimetal with a zero energy gap. In a similar way, as a result of the defect incorporation there may be obtained semiconductor – semiconductor heterojunctions with various magnitudes of the energy gap [26, 134]. Thus, a nanotube with the incorporated defect can be considered as a metal – semiconductor heterojunction, which can be used in principle as a base for a semiconductor device of record little sizes. The problem of the defect incorporation into an ideal single-layer nanotube structure meets certain technical difficulties. However it can be expected that further development of the recently created technology [71] for producing single-layer nanotubes with a specified chirality would result in the successful solution to this problem.

Possibilities for the development of highly efficient low-voltage electron field emitters and low-temperature thermal emitters on the base of nanotubes are of wide speculation in the scientific literature. These possibilities repose on the results of the above-described experiments (see Section 4.2 of this article) [27, 29, 108, 118, 119], where the intense field and thermoelectron emission were observed from both the individual nanotubes and films fabricated on their base. As stated in Ref. [118], the cross section of an electron beam emitted by an open nanotube shows up as a ring, whose diameter grows as moving away from the source of emission. So, a beam fills a space within two cones of 0.05 and 0.2 rad angles, correspondingly. Thus, the open nanotube acts as a field electron microscope with the magnification ratio as large as one million.

Possible applications of nanotubes in electronics go beyond areas related to the development of new types of diminutive elements for electronic circuits. Along with that the nanotubes can serve as a base for the finest measuring instruments used in controlling surface nonuniformities for these elements. The first possibility of such a kind was shown recently by Smalley et al. [30], using a multilayer nanotube as a probe for studying a surface at a nanometer level. The merits of usage of carbon nanotubes for this purpose are related to their extraordinary high mechanical strength, which is specifically evidenced by the directly measured data [135]. In accordance with these measurements, the Young's modulus of a nanotube in an axial direction reaches about 7000 GPa, whereas for the steel and iridium, which are used conventionally as a material for fabricating such probes, this magnitude comes to 200 and 520 GPa, correspondingly.

For fabrication of a probe in work [30], a closed from one end nanotube 5 – 20 nm in diameter and about 1 μm in length was attached to a conventional silicon cantilever with an acrylic adhesive. This permits the nanotube to be bent away whenever the tip touches a hard surface and then to snap back to its original straight position when the tip is withdrawn. The advantages of a nanotube usage as a base for a probe are defined by their unique mechanical properties, by virtue of which a nanotube aligned normally to a hard surface is bent only if the force exceeds the certain magnitude determined by the Euler formula. The tested surface was studied using a standard method in the 'tapping mode' on a frequency of about 250 kHz. The preliminary experiments showed that the nanotube-based probe owing to its small transverse size permits the penetration into trenches on the surface of a sample studied as little as 0.4 μm in width and 0.8 μm in depth, previously inaccessible to high-resolution scanning probes. Besides that, applying a pulse of the voltage to the nanotube, it could be managed to suite a carbon spot 40 nm in lateral size onto the bottom of a trench, whose image was then displayed on a monitor. In the course of preliminary experiments there was shown that not only multilayer nanotubes but also single-layer ones can be used as probes. This possibility starts from the conductive properties of nanotubes, owing to which on approaching the nanotube tip (exposed to a negative potential) to a conductor surface for a distance of 10 – 50 nm results in an electric discharge pulse, easily detectable with corresponding apparatus. Conductive properties of nanotubes permit us to rely also on their usage as a base for the scanning tunnel microscope. Already first experiments [30] performed along this line showed the possibility for obtaining the image of charge density distribution over a freshly cleaned TaS_2 surface.

5.3 Applications of nanotubes filled with various materials

A wide range of possibilities for various applications of nanotubes is related to the development and realization of methods for filling nanotubes with various materials. In doing so a nanotube can be used both as a carrier of the material filling it and as an insulating envelope, preserving a material of interest from either the electrical contact or chemical interaction with ambient objects. One of the examples dealing with the usage of nanotubes as a storage for gaseous hydrogen is given in work [91] and considered in detail above (see Section 3.3 of this article). The practical realization of this development can promote the design of a highly efficient ecologically safe car transport using the hydrogen fuel.

The possibility of the nanotube usage for insulating and storage of radioactive wastes is also the subject of wide speculation in the current literature. The merits of this storage method imply that a radioactive material encapsulated inside a nanotube is chemically inert and should not be washed out with an underground water from the storage. Thus, we can rely on an enhanced safe of this method for material keeping in comparison with conventional ones, accompanied by a considerable leakage of radioactive materials.

Researchers repose great hopes on the development of the technology of producing nanoconductors encapsulated inside single-layer nanotubes. The solution to this problem as well as to related problems of fabricating electronic circuits on the base of such conductors, can result in the lowering by 1 – 2 orders of magnitude of the minimum size of elements for microelectronic devices and, finally, in the next advance in the technologies of information processing and transmitting.

6. Conclusions

The discovery of carbon nanotubes is related to the most considerable achievements of the contemporary science. This carbon modification is intermediate in its structure between the graphite and fullerenes. However, many properties of carbon nanotubes have nothing common with neither graphite nor fullerenes. It permits the consideration and study of nanotubes as an original substance, having the unique physical and chemical characteristics.

The investigations of carbon nanotubes are of substantial basic and applied interest. The basic interest to this object is caused firstly by its unusual structure and physical and chemical properties varied over a wide range, depending on their chirality. Many of these properties serve up till now as a

subject of intense investigations directed to the determination of new interesting peculiarities in behaviour of nanotubes in one specified situation or another. There are still waiting for their solution the problems relating to the statement of the growth mechanism for carbon nanotubes in various experimental conditions, to the nature of their magnetic properties, to the degree of electron localization in pure and intercalated nanotubes, etc.

The problem of applied usage of nanotubes is closely adjacent to the problem of studying their basic properties. The solution to the former in its turn depends on the nanotube production price exceeding notably at the moment that for gold, which apparently excludes a possibility of large scale application of this material. Nevertheless such properties of nanotubes as extra tiny size, good conductivity, high emission characteristics, good chemical stability in the presence of considerable porosity and ability to join various chemical radicals permit us to hope for effective applications of nanotubes in such fields as measuring engineering, electronics and nanotechnologies, chemical technologies, etc. In the case of successful solution to these problems we shall witness to one more impressive example of the effective influence of basic research on the scientific and technological development.

The author is indebted to B M Smirnov for helpful considerations and also to the Russian Foundation for Basic Research for the partial support of this work.

References

1. Kroto H W et al. *Nature* (London) **318** 162 (1985)
2. Kraetschmer W et al. *Nature* (London) **347** 354 (1990)
3. Eletskiĭ A V, Smirnov B M *Usp. Fiz. Nauk* **163** (2) 33 (1993) [*Sov. Phys. Usp.* **36** 202 (1993)]; **165** (9) 977 (1995) [*Phys. Usp.* **38** 935 (1995)]
4. Iijima S *Nature* (London) **354** 56 (1991)
5. Mintmire J W, Dunlap B I, White C T *Phys. Rev. Lett.* **68** 631 (1992)
6. Ebbesen T W, Ajayan P M *Nature* (London) **358** 220 (1992)
7. Ebbesen T W et al. *Chem. Phys. Lett.* **209** 83 (1993)
8. Tsang S C, Harris P J F, Green M L H *Nature* (London) **362** 520 (1993)
9. Ebbesen T W et al. *Nature* (London) **367** 519 (1994)
10. Jose-Yacaman M et al. *Appl. Phys. Lett.* **62** 657 (1993)
11. Ball P *Nature* (London) **382** 207 (1996)
12. Hsu W K et al., in *Fullerenes and Fullerene Nanostructures* (Eds H Kuzmany et al.) (Singapore: World Scientific, 1996) p. 226
13. Hsu W K et al. *Chem. Phys. Lett.* **262** 161 (1996)
14. Hsu W K et al. *Nature* (London) **377** 687 (1995)
15. Ajayan P M, Iijima S *Nature* (London) **361** 333 (1993)
16. Yosida Y *Appl. Phys. Lett.* **64** 3048 (1994)
17. Saito R et al. *Appl. Phys. Lett.* **60** 2204 (1992)
18. Charlier J C, Michenaud J-P *Phys. Rev. Lett.* **70** 1858 (1993)
19. White C T, Robertson D H, Mintmire J W *Phys. Rev. B* **47** 5485 (1993)
20. Mintmire J W et al. *Mater. Res. Soc. Symp. Proc.* **247** 339 (1992)
21. Hamada N, Sawada S, Oshiyama A *Phys. Rev. Lett.* **68** 1579 (1992)
22. Mintmire J W, Dunlap B I, White C T *Phys. Rev. Lett.* **68** 631 (1992)
23. Tanaka K et al. *Chem. Phys. Lett.* **191** 469 (1992)
24. Harigaya K *Phys. Rev. B* **45** 12017 (1992)
25. Chico L et al. *Phys. Rev. Lett.* **76** 971 (1996)
26. Saito R, Dresselhaus M S, Dresselhaus G *Phys. Rev. B* **53** 2044 (1996)
27. De Heer W et al., in *Fullerenes and Fullerene Nanostructures* (Eds H Kuzmany et al.) (Singapore: World Scientific, 1996) p. 215
28. Rinzler A G et al. *Science* **269** 1550 (1995)
29. Chernozatonskiĭ L A et al. *Chem. Phys. Lett.* **233** 63 (1995)
30. Dai H et al. *Nature* (London) **384** 147 (1996)
31. Tsang S C et al., in *Fullerenes and Fullerene Nanostructures* (Eds H Kuzmany et al.) (Singapore: World Scientific, 1996) p. 250
32. Ebbesen T W et al. *Chem. Phys. Lett.* **209** 83 (1993)
33. Ajayan P M, Iijima S *Nature* (London) **358** 23 (1992)
34. Colbert D T et al. *Science* **266** 1218 (1994)
35. Ebbesen T W *Ann. Rev. Mater. Sci.* **24** 235 (1994)
36. Ebbesen T W *Phys. Today* **49** (6) 26 (1996)
37. Dravid V P et al. *Science* **259** 1601 (1993)
38. Imamura M et al. *Jpn. J. Appl. Phys.* Pt. 2 **33** L1016 (1994)
39. Zhang H et al. *J. Phys. D* **30** L1 (1997)
40. Tsang S C, Harris P J F, Green M L H *Nature* (London) **362** 520 (1993)
41. Tsang S C et al. *Nature* (London) **372** 159 (1994)
42. Ajayan P M et al. *Nature* (London) **362** 522 (1993)
43. Davis W R, Slawson R J, Rigby G R *Nature* (London) **171** 756 (1953)
44. Sacco A et al. *J. Catal.* **85** 224 (1984)
45. Speck J S, Endo M, Dresselhaus M S *J. Cryst. Growth* **94** 834 (1989)
46. Rodriquez N M, Kim M S, Baker R T K *J. Catal.* **144** 93 (1993)
47. Subramoney S et al. *Nature* (London) **366** 637 (1993)
48. Saito Y et al. *J. Appl. Phys.* **80** (5) 3062 (1996)
49. Ajayan P M et al. *Phys. Rev. Lett.* **72** 1722 (1994)
50. Ajayan P M et al. *Chem. Phys. Lett.* **215** 509 (1993)
51. Bethune D S et al. *Nature* (London) **363** 605 (1993)
52. Saito Y et al. *J. Phys. Chem. Solids* **54** 1849 (1993)
53. Saito Y et al. *Chem. Phys. Lett.* **212** 379 (1993)
54. Iijima S, Ichihashi T *Nature* (London) **363** 603 (1993)
55. Ohkohchi M et al. *Jpn. J. Appl. Phys.* **32** L1248 (1993)
56. Saito Y et al. *Jpn. J. Appl. Phys.* Pt. 2 **33** L186 (1993)
57. Ruoff R S et al. *Science* **259** 346 (1993)
58. Tomita M, Saito Y, Hayashi T *Jpn. J. Appl. Phys.* Pt. 2 **32** L280 (1993)
59. Ata M et al. *Jpn. J. Appl. Phys.* Pt. 1 **32** 3549 (1993)
60. Ugarte D *Chem. Phys. Lett.* **209** 99 (1993)
61. Ata M et al. *Jpn. J. Appl. Phys.* Pt. 1 **33** (7A) 4032 (1994)
62. Bandow S, Saito Y *Jpn. J. Appl. Phys.* Pt. 2 **32** L1677 (1993)
63. Yosida Y *Appl. Phys. Lett.* **62** 3447 (1993)
64. Majetich S A et al. *Phys. Rev. B* **48** 16845 (1993)
65. Seraphin S et al. *Appl. Phys. Lett.* **63** 2073 (1993)
66. Saito Y et al. *J. Phys. C* **98** 6696 (1994)
67. Oberlin A, Endo M *J. Cryst. Growth* **32** 335 (1976)
68. Seraphin S, Zhou D *Appl. Phys. Lett.* **64** 2087 (1994)
69. Guo T et al. *J. Phys. Chem.* **99** 10694 (1995)
70. Guo T et al. *Chem. Phys. Lett.* **243** 49 (1995)
71. Thess A et al. *Science* **273** 483 (1996)
72. Jouret C et al. *Nature* **388** 756 (1997)
73. Fischer J E *Phys. Rev. B* **55** R4921 (1997)
74. Fonseca A et al. *J. Molec. Catal. A: Chemical* **107** 159 (1996)
75. Jose-Yacaman M et al. *Appl. Phys. Lett.* **62** 657 (1993)
76. Zhang X B et al. *Europhys. Lett.* **27** (2) 141 (1994)
77. Ivanov V et al. *Chem. Phys. Lett.* **223** 329 (1994)
78. Amelinckx S et al. *Science* **265** 635 (1994)
79. Bernaerts D et al. *Philos. Mag. A* **71** 605 (1995)
80. Biro L P et al. *Proc. 11th Int. Winterschool on Electronic Properties of Novel Materials* (Kirchberg, Austria, 5–12 March 1997)
81. Bernaerts D et al., in *Physics and Chemistry of Fullerenes and Derivatives* (Eds H Kuzmany et al.) (Singapore: World Scientific, 1995) p. 551
82. Dresselhaus M S *Nature* (London) **358** 195 (1992)
83. Pederson M R, Broughton J Q *Phys. Rev. Lett.* **69** 2689 (1992)
84. Dujardin E et al. *Science* **265** 1850 (1994)
85. Ebbesen T W *J. Phys. Chem. Solids* **57** 951 (1996)
86. Tsang S C et al. *Nature* (London) **372** 159 (1994)
87. Tsang S C et al. *J. Chem. Soc. Chem. Commun.* N 1803 (1995)
88. Zhang G L et al. *J. Appl. Phys.* **80** 579 (1996)
89. Loiseau A *Fullerene Science and Technology* **4** (6) 1263 (1996)
90. Guerret-Piecourt C et al. *Nature* (London) **372** 761 (1994)
91. Dillon A C et al. *Nature* (London) **386** 377 (1997)
92. Lee R S et al. *Nature* (London) **388** 255 (1997)
93. Baxendale M et al. *Carbon* **34** 1301 (1996)
94. Mordkovich V Z et al., in *New Horizons of p-Electron Materials* (Berlin: Springer-Verlag, 1997)
95. Yudasaka M et al. *Appl. Phys. Lett.* **67** 2477 (1995)

96. Ruoff R S et al. *Nature* (London) **364** 514 (1993)
97. Zhou O et al. *Science* **263** 1744 (1994)
98. Liu M, Cowley J M *Carbon* **32** (3) 393 (1994)
99. Liu M, Cowley J M *Ultramicroscopy* **53** 333 (1994)
100. Kosaka M et al. *Chem. Phys. Lett.* **233** 47 (1995)
101. Hiura H et al. *Nature* (London) **367** 148 (1994)
102. Bursill L A, Peng J-L, Fan X-D *Philos. Mag. A* **71** 1161 (1995)
103. Howard J B, Chowdhury K D, Van der Sande J B *Nature* (London) **370** 603 (1994)
104. Weldon D N, Blau W J, Zandlbergen H W *Chem. Phys. Lett.* **241** 365 (1995)
105. Ge M, Sattler K *Science* **260** 515 (1993)
106. Yorikawa H, Muramatsu S *Phys. Rev. B* **50** 12203 (1994)
107. Cowley J M et al. *Chem. Phys. Lett.* **265** 379 (1997)
108. De Heer W A, Chatelain A, Ugarte D *Science* **370** 1179 (1995)
109. De Heer W A et al. *Science* **268** 845 (1995)
110. Langer L et al. *Phys. Rev. Lett.* **76** 479 (1996)
111. Langer L et al. *J. Mater. Res.* **9** 927 (1994)
112. Langer L et al., in *Physics and Chemistry of Fullerenes and Derivatives* (Eds H Kuzmany et al.) (Singapore: World Scientific, 1995) p. 565
113. Ajiki H, Ando T *J. Phys. Soc. Jpn.* **62** 1255 (1993)
114. Song S N et al. *Phys. Rev. Lett.* **72** 697 (1994)
115. Ebbesen T W et al. *Nature* (London) **382** 54 (1996)
116. Primak W, Fuchs L H *Phys. Rev.* **95** 22 (1954)
117. Tans S J et al. *Nature* (London) **386** 474 (1997)
118. Saito Y et al. *Nature* **389** 554 (1997)
119. Gulyaev Yu V et al. *Mikroelektronika* **26** (2) 84 (1997)
120. Chauvet O et al. *Phys. Rev. B* **52** R6963 (1995)
121. Ramirez A P et al. *Science* **265** 84 (1994)
122. Baxendale M et al. *Proc. 11th Int. Winterschool on Electronic Properties of Novel Materials* (Kirchberg, Austria, 5 – 12 March 1997) Rep. PSI-3
123. Luo W et al. *Bull. Am. Phys. Soc.* **39** 758 (1994)
124. Dresselhaus M S, Dresselhaus G *Adv. Phys.* **30** 139 (1981)
125. Ramirez A P et al. *Science* **265** 84 (1994)
126. Heremans J, Olk C H, Morelli D T *Bull. Am. Phys. Soc.* **39** 897 (1994)
127. Li Z G, Fagan P F, Report ICEM-13, Paris 1994
128. Planeix J M et al. *J. Am. Chem. Soc.* **116** 7935 (1994)
129. Ajayan P M et al. *Nature* (London) **375** 564 (1995)
130. Niu C et al. *Appl. Phys. Lett.* **70** 1480 (1997)
131. Wang K et al. *Chinese Science Bull.* **40** 1245 (1995)
132. Huira H, Ebbesen T W, Tanigaki K *Adv. Mater.* **7** 275 (1995)
133. Chico L et al. *Phys. Rev. Lett.* **76** 971 (1996)
134. Dresselhaus M S, Dresselhaus G, Eklund P C *Science of Fullerenes and Nanotubes* (San Diego: Academic Press, 1996)
135. Zettl A, Chopra N G, in *Fullerenes and Fullerene Nanostructures* (Eds H Kuzmany et al.) (Singapore: World Scientific, 1996) p. 232
136. scss A M et al. *Nature* (London) **388** 257 (1997)